

Toward an internally consistent astronomical distance scale

Richard de Grijs, Frédéric Courbin, Clara E. Martínez-Vázquez, Matteo Monelli, Masamune Oguri, and Sherry H. Suyu

Received: date / Accepted: date

Abstract Accurate astronomical distance determination is crucial for all fields in astrophysics, from Galactic to cosmological scales. Despite, or perhaps because of, significant efforts to determine accurate distances, using a wide range of methods, tracers, and techniques, an internally consistent astronomical dis-

Richard de Grijs

Kavli Institute for Astronomy & Astrophysics and Department of Astronomy, Peking University, Yi He Yuan Lu 5, Hai Dian District, Beijing 100871, China

E-mail: grijs@pku.edu.cn;

International Space Science Institute–Beijing, 1 Nanertiao, Zhongguancun, Hai Dian District, Beijing 100190, China

Frédéric Courbin

Institute of Physics, Laboratoire d’Astrophysique, Ecole Polytechnique Fédérale de Lausanne (EPFL), Observatoire de Sauverny, CH-1290 Versoix, Switzerland

E-mail: frederic.courbin@epfl.ch

Clara E. Martínez-Vázquez

Instituto de Astrofísica de Canarias, Calle Vía Láctea sn, 38205 La Laguna, Spain

Universidad de La Laguna (ULL), Dpto. Astrofísica, E-38206 La Laguna, Tenerife, Spain

E-mail: clara.marvaz@gmail.com

Matteo Monelli

Instituto de Astrofísica de Canarias, Calle Vía Láctea sn, 38205 La Laguna, Spain;

Universidad de La Laguna (ULL), Dpto. Astrofísica, E-38206 La Laguna, Tenerife, Spain

E-mail: monelli@iac.es

Masamune Oguri

Department of Physics, Graduate School of Science, University of Tokyo, 7-3-1 Hongo, Bunkyo-ku, Tokyo 113-0033, Japan

E-mail: masamune.oguri@ipmu.jp

Sherry H. Suyu

Max-Planck-Institut für Astrophysik, Karl-Schwarzschild-Str. 1, 85748 Garching, Germany

E-mail: suyu@mpa-garching.mpg.de;

Institute of Astronomy and Astrophysics, Academia Sinica, P.O. Box 23-141, Taipei 10617, Taiwan;

Physik-Department, Technische Universität München, James-Frank-Straße 1, 85748 Garching, Germany

tance framework has not yet been established. We review current efforts to homogenize the Local Group’s distance framework, with particular emphasis on the potential of RR Lyrae stars as distance indicators, and attempt to extend this in an internally consistent manner to cosmological distances. Calibration based on Type Ia supernovae and distance determinations based on gravitational lensing represent particularly promising approaches. We provide a positive outlook to improvements to the status quo expected from future surveys, missions, and facilities. Astronomical distance determination has clearly reached maturity and near-consistency.

Keywords gravitational lensing: strong – stars: distances – stars: variables: RR Lyrae — Galaxy: center – Galaxy: fundamental parameters – galaxies: distances and redshifts – Local Group – Magellanic Clouds – distance scale

1 Introduction

Distance determination from the nearest stars to the edge of the observable Universe crucially depends on accurate calibration of every successive rung of the so-called astronomical ‘distance ladder’ (for a modern version of the distance ladder, see de Grijs, 2013). Local benchmark objects often used to optimally constrain the uncertainties inherent to using a stepwise calibration approach include the distances to the Galactic Center and a number of well-studied galaxies in the Local Group.

R_0 , the distance from the solar circle to the Galactic Center is particularly instrumental to achieve a basic calibration for a wide range of methods used for distance determination, across an extensive range of distance scales. Among other key physical parameters, the distances, masses, and luminosities of Galactic objects, as well as the Milky Way’s total mass and luminosity, depend directly on knowing R_0 accurately. For instance, most luminosity and a large number of mass estimators scale as R_0^2 , whereas masses based on total densities or orbital modeling scale as R_0^3 .

This intrinsic dependence therefore often requires adoption of an integrated mass and/or a rotation model for the Milky Way, which in turn would also require us to accurately know the Sun’s circular velocity, Θ_0 . As R_0 estimates are refined, so are the estimated distances, masses, and luminosities of numerous Galactic and extragalactic objects, as well as our best estimates of the rate of Galactic rotation and the size of the Milky Way. In addition, a highly accurate direct Galactic Center distance determination is paramount for a reliable recalibration of the zero points of numerous commonly used distance calibrators, including of Cepheids, RR Lyrae (see below), and Mira variable stars.

Beyond Galactic distance tracers, distance measurements to the Large Magellanic Cloud (LMC) have played an important role in constraining the value of the Hubble constant, H_0 . The ‘*Hubble Space Telescope (HST) Key Project (HSTKP) on the Extragalactic Distance Scale*’ (Freedman et al., 2001) resulted in an H_0 estimate of $H_0 = 72 \pm 3$ (statistical) ± 7 (systematic) km s^{-1}

Mpc^{-1} . The latter, systematic uncertainty was thought to be dominated by the remaining systematic uncertainties in the assumed distance to the LMC (Freedman et al., 2001; Schaefer, 2008; Pietrzyński et al., 2013), which contributed of order $\pm 3\text{--}4 \text{ km s}^{-1} \text{ Mpc}^{-1}$ to the tally.

On a number of occasions, the accuracy of LMC distance determinations has been called into question by claims of ‘publication bias’ (e.g., Schaefer, 2008, 2013; Rubele et al., 2012; Walker, 2012). Therefore, in de Grijs et al. (2014) we re-analyzed the full body of LMC distance measurements published between 1990 and 2013, embarking on the most extensive data-mining effort of this type done to date. Perhaps somewhat surprisingly, we concluded that strong publication bias is unlikely to have been the main driver of the clustering of many published LMC distance moduli. However, we found that many of the published values were based on highly non-independent tracer samples and analysis methods. In turn, this interdependence appears to have led to significant correlations among the body of LMC distances we considered in de Grijs et al. (2014). Our final, recommended true distance modulus for the LMC is $(m - M)_0 = 18.49 \pm 0.09 \text{ mag}$ (de Grijs et al., 2014, see also Crandall and Ratra 2015). In an effort to provide a firm mean distance estimate to the Small Magellanic Cloud (SMC), and thus place it within the internally consistent Local Group distance framework (that is, a distance framework where all combinations of distances lead to the same underlying scaling), de Grijs and Bono (2015) similarly performed extensive analysis of the published literature to compile the largest database available to date containing SMC distance estimates. For the first time, we provided estimates of the mean SMC distance based on large numbers of distance tracers, without imposing any a priori preferences. We derived a true distance modulus of $(m - M)_0^{\text{SMC}} = 18.96 \pm 0.02$, corresponding to a distance of $61.9_{-0.5}^{+0.6} \text{ kpc}$.

Indeed, the nearest galaxies in the Local Group contain numerous objects that can be used to determine robust distances, that is, distances with well-defined uncertainties that are mutually consistent among the different tracers. In de Grijs et al. (2014), de Grijs and Bono (2014), de Grijs and Bono (2015), and de Grijs and Bono (2016), we aimed at establishing an internally consistent local distance framework by reference to the subset of distances to the Galactic Center, the LMC and SMC, M31, M32, and M33, as well as a number of well-known dwarf galaxies. We aimed at reaching consensus on the best, most homogeneous, and internally most consistent set of Local Group distance moduli.

At the present time, we are in a good position to make recommendations for the use of robust distance measurements to a set of key Local Group galaxies: see Table 1 and Fig. 1.

In this review, we will first consider the distances to the Galactic Center as well as to a select number of Local Group galaxies resulting from large-scale data mining of the literature (Sections 1–3). Our aim is to establish an internally consistent distance framework in the Local Group using multiple, independent methods. We will then proceed to review the distances to Local Group galaxies based specifically on space-based data of variable stars,

Table 1 Internally consistent distance moduli (as a function of increasing distance) to selected Local Group galaxies, comprising a robust local framework (adapted from de Grijs and Bono, 2015).

Galaxy	$(m - M)_0^{\text{best}}$ (mag)	Tracer(s)	$(m - M)_0^{\text{TRGB}}$ (mag)
LMC	18.49 ± 0.09	Cepheids, RR Lyrae, CMD	18.54–18.69
SMC	18.96 ± 0.02	EBs, Cepheids, RR Lyrae, TRGB, RC	19.00 ± 0.04
NGC 185	24.00 ± 0.12	TRGB, RR Lyrae	24.03 ± 0.33
NGC 147	24.11 ± 0.11	TRGB, RR Lyrae	24.16 ± 0.22
IC 1613	24.34 ± 0.05	Cepheids, RR Lyrae, TRGB	24.29 ± 0.12
IC 10	24.36 ± 0.45	TRGB	24.36 ± 0.45
M32	24.43 ± 0.07	SBF, TRGB, RR Lyrae	24.32 ± 0.20
M31	24.45 ± 0.10	Cepheids, RR Lyrae, TRGB	24.47 ± 0.01
NGC 205	24.56 ± 0.15	TRGB, RR Lyrae	24.45 ± 0.20
M33	24.67 ± 0.07	Cepheids, RR Lyrae, TRGB	24.70 ± 0.11
NGC 4258	29.29 ± 0.08	H ₂ O masers	29.24–29.44

Notes: CMD: color–magnitude diagram; EBs: eclipsing binaries; RC: red clump; SBF: surface-brightness fluctuations; TRGB: tip of the red giant branch.

with emphasis on the uniformity in distance measurement across the nearby galaxies afforded by RR Lyrae stars (Sections 4–6). Local Group RR Lyrae represent a powerful tool, because they are found in old stellar populations that are present in galaxies of any Hubble type and luminosity class (with the possible exception of the ultra-faint dwarf galaxies). We will discuss a large number of case studies aimed at their internally consistent calibration as a single, homogenized distance indicator well beyond the Local Group. At greater distances, we focus on efforts to obtain improved distances and particularly on a number of alternate techniques to constraining the Hubble constant (Section 7), with particular emphasis on gravitational lensing as a promising tool (Section 8). The resulting distances not cross-calibrations of other distance indicators; instead, they encompass a derived quantity—the Hubble law—from which distances are computed.

We emphasize that an internally consistent distance scale exists, for a given cosmology, naturally in the Hubble flow owing to the relationship between distance and redshift. On these cosmological scales, the key to consistency is therefore not distance as such, but re-enforcing the cosmological parameters from which these distances are derived. At the present time, these cosmological parameters are predominantly derived on the basis of observations of Type Ia supernovae (SNe Ia) and the cosmic microwave background. Our discussion in Sections 7 and 8 focuses on alternative means of measuring the Hubble constant, not necessarily on the objects’ specific distances. Therefore, gravitational lensing and galaxy cluster-based techniques are not direct cross-checks on the SNe Ia-derived distances, but on the Hubble constant measured from SNe Ia. The latter distance framework is currently calibrated on the basis of Cepheid distances, which are directly tied into the internally consistent distance scales discussed in Sections 1–3.

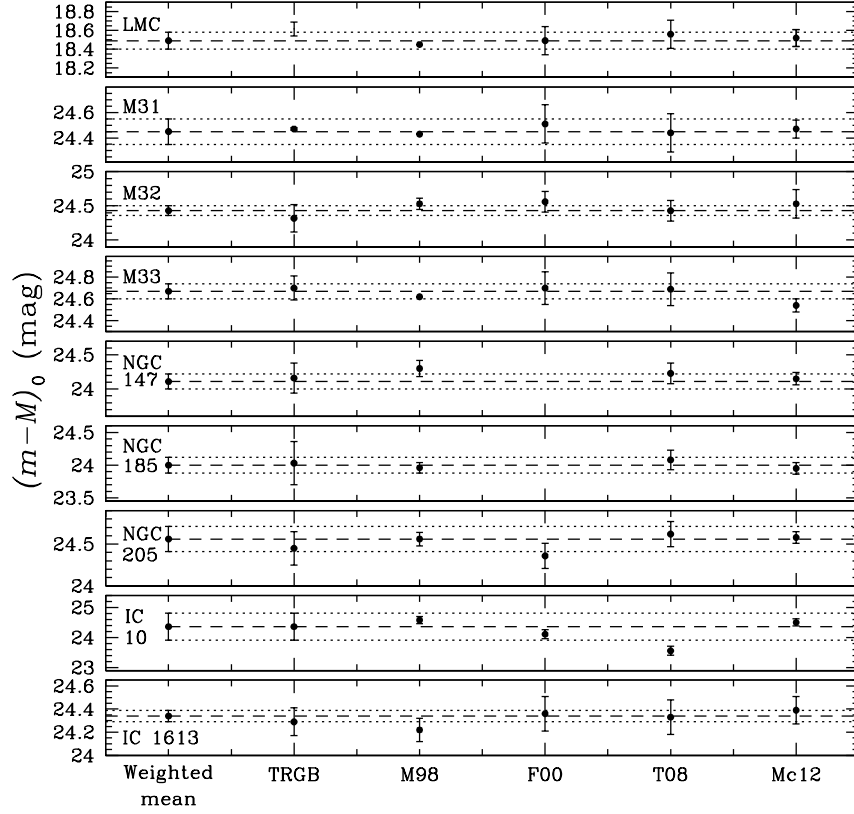


Fig. 1 Comparison of our set of benchmark distances to the sample of Local Group galaxies (indicated in the individual panels) discussed in this article with those from a number of recent distance compilations. ‘Weighted mean’ and TRGB: de Grijs and Bono (2015), except where indicated in Table 1; M98: Mateo (1998); F00: Ferrarese et al. (2000); T08: Tammann et al. (2008); Mc12: McConnachie (2012). From de Grijs and Bono (2015).

2 Distance to the Galactic Center

In recent years various authors have speculated that some degree of publication bias may have affected Galactic Center distance determinations (e.g., Reid, 1989, 1993; Nikiforov, 2004; Foster and Cooper, 2010; Malkin, 2013a,b; Francis and Anderson, 2014). Aiming at deriving a statistically well-justified Galactic Center distance based on a large variety of tracers and reducing any occurrence of publication bias, de Grijs and Bono (2016) therefore undertook an extensive data-mining effort of the literature.

They separated the compilation of R_0 determinations into direct and indirect distance measurements. The former include distances such as those based

on orbital modeling of the ‘S stars’ orbiting Sgr A*, the closest visual counterpart of the Milky Way’s central supermassive black hole, as well as those relying on statistical parallaxes of Galactic Center tracers. Careful assessment of the body of published R_0 estimates based on these methods resulted in a Galactic Center distance recommendation of $R_0 = 8.3 \pm 0.2$ (stat.) ± 0.4 (syst.) kpc.

A much larger body of Galactic Center distance determinations is based on indirect methods, either relying on determinations of the centroids defined by the three-dimensional distributions of a range of different tracer populations (e.g., globular clusters, Cepheid, RR Lyrae, or Mira variables, or red clump stars) or measurements based on kinematic observations of objects at the solar circle. The latter approaches are affected by significantly larger uncertainties than the former; the central, mean Galactic Center distances based on the kinematic methods are systematically smaller than those based on centroid determinations. Most centroid-based distances are in good agreement with those resulting from the direct methods. de Grijs and Bono (2016) did not find any conclusive evidence of the presence of publication bias in the post-1990 R_0 measurements.

3 Internally consistent distances to the Magellanic Clouds

As the nearest, irregular galaxies to our Milky Way, the Magellanic Clouds represent the first, important rung of the extragalactic distance ladder. They cover sizeable areas on the sky, thus providing access to large samples of tracer objects. For instance, the VISTA Survey of the Magellanic Clouds Cioni et al. (2011), which covers the LMC, the SMC, the Magellanic Bridge, and a few fields in the Magellanic Stream, is in currently the process of compiling a 184 deg² mosaicked map of the entire system.

Indeed, the LMC is the nearest extragalactic environment that hosts statistically significant samples of the tracer populations for distance determination, such as Cepheid and RR Lyrae variable stars, eclipsing binaries (EBs), and red-giant-branch (RGB) stars, as well as supernova (SN) 1987A. These could thus potentially link the local (i.e., solar-neighborhood and Galactic) tracers to their counterparts in more distant and more poorly resolved galaxies. At a distance of approximately 50 kpc, the LMC represents the only well-studied environment linking Galactic distance tracers to those in other large spiral and elliptical galaxies at greater distances. Its three-dimensional, thin disk-like morphology renders it an ideal target galaxy where off-center distances can easily be projected onto the galaxy’s center through simple projection.

Lingering systematic uncertainties remain in the distance to the LMC. This has obvious ramifications in the context of using the LMC distance as a calibrator, specifically to reduce the uncertainties in the Hubble constant (cf. Freedman et al., 2001; Schaefer, 2008; Pietrzyński et al., 2013). Although this has also led to persistent claims of ‘publication bias’ affecting published distances to the galaxy (cf. Schaefer, 2008, 2013; Rubele et al., 2012; Walker,

2012), de Grijs et al. (2014) made a case of highly correlated results rather than publication bias. Nevertheless, the LMC distance moduli is common use today are likely still affected by poorly understood systematic uncertainties.

Fortunately, the LMC is sufficiently close that some geometric distance tracers are readily available, including an increasing sample of EB systems. Highly promising, Pietrzyński et al. (2013) determined the direct distances to eight late-type EB systems in the LMC, resulting in an average distance modulus of $(m - M)_0 = 18.493 \text{ stat.} \pm 0.008 \pm 0.047 \text{ (syst.) mag}$. This value is accurate to 2.2% and confirms that the statistically justified distance modulus of $(m - M)_0 = 18.49 \pm 0.09$ is indeed reasonable. Pietrzyński et al. (2013) discovered giant stars in EB systems, which uniquely allowed them to use the very well calibrated surface-brightness- $(V - K)$ color relation for such stars to determine their angular sizes, so that their error estimates are more robust and reproducible, and less affected by lingering systematic effects than competing results based on early-type EBs. Some of the most recent analyses, e.g., Inno et al. (2016)’s study of the three-dimensional distribution of classical Cepheids in the LMC’s disk, have derived true distance moduli that are in excellent agreement with both the statistical average and the geometric distance determination of Pietrzyński et al. (2013).

In this context it is important to note that Riess et al. (2016) recently used Cepheid distances to independently obtain an internally consistent distance framework including the Milky Way, the LMC, M31, and the maser host galaxy NGC 4258. This underscores the importance of the LMC as the lowest rung of the extragalactic distance ladder, and this also links the local distance framework naturally to our discussion of derivations of the Hubble constant in Section 7 and beyond, particularly those based on SNe Ia observations.

de Grijs and Bono (2015) performed a similar analysis for the SMC as they did for the LMC. Obtaining a clear-cut distance to the SMC is not as straightforward as for the LMC, however. First, given the SMC’s bar-like main body with hints of spiral arms and a very extended ‘Wing’ to the East, defining the position of the galaxy’s center is troublesome. Rubele et al. (2015) recently derived distances to different areas across the galaxy. They report distances projected onto both the SMC’s kinematic and stellar density centers, $(m - M)_0^{\text{kin}} = 18.97 \pm 0.01 \text{ mag}$ and $(m - M)_0^{\text{stars}} = 18.91 \pm 0.02 \text{ mag}$, respectively. This implies that the choice of SMC center could introduce systematic uncertainties of order 0.05–0.1 mag in the resulting distance modulus.

Second, the SMC is very extended along the line of sight. Its depth could range from 6–12 kpc (Crowl et al., 2001) up to 20 kpc (Groenewegen, 2000, for recent discussions, see e.g., Kapakos and Hatzidimitriou 2012; Subramanian and Subramanian 2012; Cignoni et al. 2013; Kalirai et al. 2013; Nidever et al. 2013; Scowcroft et al. 2016), although the Cepheid population associated with the main body implies a shallower depth of $1.76 \pm 0.6 \text{ kpc}$ (Subramanian and Subramanian, 2015). (Scowcroft et al., 2016) recently also used Cepheids to study the SMC’s line-of-sight depth, but based on observations in nine photometric passbands simultaneously, including four near- to mid-infrared *Spitzer Space Telescope* filters. They confirmed that the Cepheid distribution is inconsistent with a

significant depth, although they pointed out that the southwestern side of the galaxy is up to 20 kpc more distant than the SMC’s northeast.

Third, the SMC’s measured inclination appears to depend on the stellar tracer (and thus the age of the stellar population) used (Caldwell and Coulson, 1986; Laney and Stobie, 1986; Groenewegen, 2000; Haschke et al., 2012; Subramanian and Subramaniam, 2012; Rubele et al., 2015). Careful geometric corrections of individual objects back to the galaxy’s center will reduce the scatter in the calibration relations, but this is not always possible. A warped disk (the presence of which is still debated) will introduce additional systematic uncertainties, of order 0.1 in the distance modulus (de Grijs and Bono, 2015).

de Grijs (2011, his Chapter 6.1.1) provides a detailed discussion of the systematic uncertainties associated with the effects of extinction in the context of distance determinations. These include uncertainties related to our knowledge of (i) the most likely extinction law, (ii) the intrinsic photometric properties of one’s calibration objects, and (iii) the dust geometry. The choice of extinction law is particularly important when comparing similar types of objects drawn from Galactic and Magellanic Cloud samples, since ‘the’ Galactic extinction law (which may vary along different lines of sight) differs systematically from that in the Magellanic Clouds (for recent studies, see e.g., Dobashi et al., 2009; Bot et al., 2010, and references therein). Nevertheless, the differences are generally $\lesssim 0.05$ mag at near-infrared and longer wavelengths and shortward of $\lambda = 0.8\mu\text{m}$.

4 RR Lyrae variables in the Local Group

RR Lyrae stars are low-mass ($\sim 0.6\text{--}0.8M_{\odot}$) core helium-burning stars in their horizontal-branch (HB) evolutionary phase. They are radially pulsating variable stars with periods ranging from 0.2 to 1.0 days and V -band amplitudes between 0.2 and $\lesssim 2$ mag. Their mean absolute V -band magnitude is $M_V \sim +0.6$ mag, they are of moderate brightness ($\approx 40L_{\odot}$), and their effective mean temperatures range from 6000 to 7250 K (Catelan et al., 2004). RR Lyrae stars are found in stellar systems hosting old old stellar populations ($t > 10$ Gyr; Walker, 1989; Smith, 1995; Catelan & Smith, 2015); they can currently be observed out to distances of ~ 2 Mpc (Da Costa et al., 2010; Yang et al., 2014). Additionally, RR Lyrae stars are primary distance indicators, since they obey well-defined optical/near-infrared period–luminosity relations (PLRs; see, e.g., Bono et al., 2001, 2003; Clementini et al., 2003; Catelan et al., 2004; Marconi et al., 2015, see for more details also R. Beaton et al., in prep.).

The Local Group is home two ‘normal’ spiral galaxies, the Milky Way and the Andromeda galaxy, M31, shepherded by a number of dwarf galaxies. Thanks to large photometric surveys, the number of known satellites of both systems has been increasing rapidly in the last few years (e.g. Willman et al., 2006; Martin et al., 2015, see also http://www.astro.uvic.ca/~alan/Nearby_Dwarf_Database.html). From an observational point of view, the properties of Local Group galaxies

span the most diverse ranges (Mateo, 1998; McConnachie, 2012). In particular, observational approaches to characterize the population of RR Lyrae have to be adapted to the different systems. Faint nearby galaxies (often called ‘ultra-faint dwarfs,’ with $-8 \lesssim M_V \lesssim -1.5$ mag) are characterized by extremely low surface brightnesses. They typically represent concentrations of a few hundred stars in a relatively small projected volume covering a few square arcminutes on the sky. These objects typically have low mean metallicities ($[\text{Fe}/\text{H}] \sim -2$ dex), exhibit blue HB morphology, and host very few RR Lyrae stars (e.g. Vivas et al., 2016).

On the other hand, more massive ‘classical’ dwarf satellites ($-13 \lesssim M_V \lesssim -9$ mag) are very rich in RR Lyrae stars (Kinemuchi et al., 2008; Stetson et al., 2014; Coppola et al., 2015; Martínez-Vázquez et al., 2015), but they cover large areas on the sky, up to many square degrees, and require wide-field facilities on medium-sized, ground-based telescopes for follow-up studies. At present day, a complete census and analysis of the population of variable stars, and of RR Lyrae stars in particular, is not yet available for any bright Local Group galaxy (with the possible exception of Leo I and the Carina dwarf spheroidal galaxy, Stetson et al., 2014; Coppola et al., 2015). A case in point in this context is illustrated by the monitoring of two of the most massive Milky Way satellites, the Magellanic Clouds, performed by the Optical Gravitational Lensing Experiment, which collected $\sim 45,000$ RR Lyrae variables in the Magellanic System in their latest release (Soszyński et al., 2016).

Another crucial point to bear in mind is that Local Group galaxies represent an enormous variety of intrinsic properties, e.g., in terms of their sizes, morphologies, gas content, chemical evolution, and stellar populations. As a consequence, they host a variety of families of variable stars, whose properties reflect the evolutionary history of the host system. As an example, RR Lyrae stars carry direct information of the chemical properties of the environment in which they formed during the first stages of a galaxy’s lifecycle. An intrinsic spread in metallicity in the population of RR Lyrae stars in a dwarf galaxy implies chemical enrichment which not only occurred at early times, but which was sufficiently rapid to be imprinted in the stellar population that we observe today as RR Lyrae stars (Bernard et al., 2008; Martínez-Vázquez et al., 2015). Moreover, the number of RR Lyrae stars in a galaxy depends on the level of star formation at early times. Leo A ($M_V = -12.1$ mag), which has very little early star-formation activity (Cole et al., 2007), hosts a handful of RR Lyrae stars (Bernard et al., 2013), while Sculptor ($M_V = -11.1$ mag), is a predominantly old system (de Boer et al., 2012) with a population of RR Lyrae stars that outnumbers that of Leo A by two orders of magnitude, despite the latter galaxy’s lower mass (Martínez-Vázquez et al., 2016).

RR Lyrae stars are primary distance indicators, which can be detected beyond the limits of the Local Group (Da Costa et al., 2010; Yang et al., 2014; McQuinn et al., 2015). Different methods can be applied to derive distances based on the properties of RR Lyrae stars, including (i) the luminosity–metallicity relation (LMR) in the V band, (ii) PLRs and period–Wesenheit relations (PWRs), and (iii) the First Overtone Blue Edge (FOBE) method.

Nevertheless, compiling a homogeneous set of distances to nearby galaxies using the properties of their variable stellar populations is not an easy task. Below, we summarize the main aspects which must be taken into account.

1. **Photometric calibration:** As regards data pertaining to nearby satellite galaxies, large numbers of data sets are available in the literature, collected over decades by different observers with different telescopes, equipped with different filters and cameras. This poses a fundamental problem to derive homogeneous photometry in a well-established system (Stetson, 2000). Photometric measurements based on *Hubble Space Telescope* (*HST*) observations are typically provided in the natural VEGAMAG photometric system, and they may be recalibrated to the Johnson–Cousins system a posteriori. However, different conversion relations have been proposed (Bedin et al., 2004; Sirianni et al., 2005; Bernard et al., 2009), many of which are affected by significant color dependences.
2. **Data quality and derivation of the pulsation parameters:** Deriving good pulsation properties for variable stars requires adequate sampling of their light curves. Especially for existing *HST* data, this is not always the case: rarely more than 25 phase points are available. The parameters derived from sparsely populated light curves may depend on the approach used for the analysis, the fitting algorithm, and/or the template adopted. Moreover, long-term and continuous monitoring of variable stars has revealed complex behavior (including period doubling, the Blazhko effect, period changes, and non-radial modes, among others) which is impossible to detect and characterize on the basis of sparsely sampled observations.
3. **The effects of metallicity:** It is worth recalling that most relations used to derive distances to RR Lyrae stars require one to assume the relevant metallicity. The only notable exceptions (Marconi et al., 2015; Martínez-Vázquez et al., 2015) are the PWR in $(V, B - V)$ and $(V, B - I)$. Marconi et al. (2015, their Tables 7 and 8) performed an elaborate analysis of optical, optical–near-infrared, and near-infrared PWRs. They found that the coefficient of the metallicity term was less than ~ 0.05 dex for the $(V, B - V)$ and $(V, B - I)$ PWRs, indicating that the V -band metallicity effects are counteracted by the convolution of the reddening vector and the $(B - V)$ or $(B - I)$ colors. Since high-resolution spectroscopy for RR Lyrae stars in external galaxies is generally not available, other indicators or methods must be established to estimate the chemical composition of RR Lyrae stars. Typically, the metallicity distribution of bright red-giant-branch (RGB) stars is available from spectroscopic studies, most commonly low-resolution calcium triplet spectra. Since different authors may use different metallicity scales or calibrations, deriving homogeneous distances is hence not a trivial task.

Moreover, RGB stars cover an age range of $\gtrsim 1.5$ Gyr, and the mix of stellar populations of different ages and metallicities is highly degenerate in color–magnitude space. The metallicity distribution derived from RGB stars is a good approximation of a galaxy’s global population, but it does not prop-

erly describe the RR Lyrae stars or the old populations (>10 Gyr). As a consequence, assuming a mean metallicity for the RR Lyrae stars that is too high would introduce a systematic error in distance-modulus estimates, at the level of ~ 0.2 mag. Therefore, assumptions have to be made regarding the RR Lyrae metallicity distribution, or alternatively this distribution must be determined based on other methods (Martínez-Vázquez et al., 2016).

4. **Calibration:** Despite its extensive use in the literature and its simple form, the LMR relation cannot yet boast a solid calibration, neither of its zero point nor of its slope. A number of different calibrations exist (Chaboyer, 1999; Bono et al., 2003; Clementini et al., 2003; Carretta et al., 2009), and using one rather than another can introduce a difference on the order of 0.2 mag in the distance determination.
5. **Reddening:** Correction for interstellar extinction is a crucial step required to derive the absolute magnitudes of one's target stars—and in turn their distance moduli. Systems with significant internal reddening may be not adequately corrected by employing any of the widely used reddening maps (Schlegel et al., 1998; Schlafly and Finkbeiner, 2011). Moreover, differential reddening introduces significant scatter in the mean magnitudes and colors of stars, which may strongly affect the analysis (e.g., see Sarajedini et al., 2006). To (at least partially) overcome this problem, one can use a Wesenheit pseudo-magnitude (van den Bergh, 1968), which is reddening-free by construction (under assumption of a reddening law), or move to near-infrared wavelengths, where the effect of extinction is strongly reduced.

RR Lyrae-based distance estimates in the literature are, therefore, not homogeneous for a large number of reasons: use of different algorithms for the photometry or of different recipes for the photometric calibration, the existence of different calibrations for the same method of distance determination, metallicities which may be defined on a different scale and/or which may not be appropriate for the sample of RR Lyrae stars, and the assumed reddening, among others. Revision of existing data in an effort to provide a homogeneous distance framework is not a trivial task either. We will next revise the data and the distance estimates available for galaxies in the M31 system, for isolated galaxies, and even to some extent for galaxies outside the Local Group. We will subsequently proceed, using already available data, to provide a homogeneous RR Lyrae-based distance framework. In particular, we will rely on data for six M31 satellite galaxies, which we use as test cases to probe the reliability of different methods, and we will also provide new distance estimates to 16 dwarf galaxies based on *HST* data.

5 RR Lyrae in the Local Group and beyond: status

The search for RR Lyrae stars in the M31 system has been long limited because of (i) their (relatively) faint apparent magnitudes ($V \sim 25$ mag) and (ii)

crowding effects. The first successful attempt to identify RR Lyrae stars in the M31 halo was achieved by Pritchett and van den Bergh (1987), using Canada–France–Hawaii Telescope data. A few years later, Saha and Hoessel (1990) and Saha et al. (1990) detected candidate RR Lyrae stars in the M31 dwarf elliptical (dE) satellites NGC 185 and NGC 147, respectively. Nevertheless, it was only thanks to the *HST* and its spatial resolution that it was possible to reach well below the HB and achieve the first solid determination of the properties of RR Lyrae stars in the M31 field and its satellites Clementini et al. (e.g., 2001).

5.1 M31 dwarf spheroidals

Based on *HST*/Wide Field and Planetary Camera-2 (WFPC2) data, in a series of papers devoted to the properties of the stellar populations in M31 dwarfs, discoveries of RR Lyrae stars were reported in And I (Da Costa et al., 1996), And II (Da Costa et al., 2000), and And III (Da Costa et al., 2002). The populations of variable stars detected in these three galaxies were later analyzed in detail by Pritzl et al. (2004, And II) and Pritzl et al. (2005a, And I and And III). Moreover, And VI was studied by Pritzl et al. (2002a) on the basis of data of comparable quality. The distances and distance moduli were derived for the four galaxies using the LMR relation of Lee (1990), assuming a mean metallicity derived from the mean color of the RGB.

Interestingly, following these pioneering studies, the number of known satellites of M31 has dramatically increased in the last 10 years, mostly thanks to the PAndAS survey McConnachie et al. (2009). However, few surveys specifically include studies of variable stars. *HST*/WFPC2 data were used by Yang and Sarajedini (2012) to study two low-mass M31 satellites, And XI and And XIII, where they detected 17 and 9 bona fide RR Lyrae candidates, respectively. Their distance moduli were derived using Chaboyer (1999)’s calibration of the LMR relation. The RR Lyrae metallicity was derived using the Alcock et al. (2000) relation, and the mean of the distribution was used to derive the distance modulus.

Other recently discovered satellites have been studied using wide-field, ground-based Large Binocular Telescope data. The results have been presented in a series of papers which discuss the RR Lyrae stellar populations in And XIX (Cusano et al., 2013), And XXI (Cusano et al., 2015), and And XXV (Cusano et al., 2015). In these studies, the authors adopted a consistent method to derive the distances to the three galaxies, based on the LMR relation calibrated by Clementini et al. (2003). In these three cases, the adopted metallicity was based on low-resolution RGB spectroscopy (Collins et al., 2013), which is reasonable for the RR Lyrae stars in these galaxies as well, given the low mass of the three galaxies.

5.2 RR Lyrae stars in the M31 field

The availability of the *HST*/Advanced Camera for Surveys (ACS) resulted in a new and significant step forward. New *HST*/ACS data targeted two of the brightest M31 satellites, M33 (Sarajedini et al., 2006) and M32 (Sarajedini et al., 2012). The metallicity of individual RR Lyrae stars was derived using a relation between $[\text{Fe}/\text{H}]$ and the period (Sarajedini et al., 2006) and a relation between $[\text{Fe}/\text{H}]$, the period, and the amplitude (Alcock et al., 2000). Once the mean metallicity of the sample was known, the distance modulus was derived assuming the LMR as calibrated by Chaboyer (1999). A similar approach was used by Fiorentino et al. (2010) and Fiorentino et al. (2012a) for M32, who used the relation of Alcock et al. (2000) to derive the metallicity distribution of their M32 sample RR Lyrae stars. However, Fiorentino et al. (2010) used two different approaches to derive the distance modulus to the galaxy. In addition to the LMR relation (Cacciari and Clementini, 2003), they also applied the FOBE method. Given the sizeable sample of RRc-type stars (first-overtone pulsators), they derived an independent distance modulus, in agreement with the other LMR method.

The most comprehensive analysis of RR Lyrae stars in M31 has been published by Jeffery et al. (2011), who analyzed different ACS fields in the galaxy’s disk and inner halo, as well as a region overlapping with the Giant Stellar Stream (GSS) that is being accreted onto M31 (Ibata et al., 2001). Jeffery et al. (2011) performed a detailed analysis of the metallicity determination based on different methods, as well as their effect on the derived distance modulus. In particular, they compared the period–metallicity relation (Sarajedini et al., 2006), the period–amplitude–metallicity relation (Alcock et al., 2000), Bono et al. (2007)’s method based on theoretical period–amplitude–metallicity relations, and the period–metallicity relation for RRc type stars (Sandage, 1993). A comparison of the metallicities derived photometrically using the first three methods with respect of spectroscopic measurements reveals good agreement between the Alcock et al. (2000) and Bono et al. (2007) methods, although the latter exhibits a significantly smaller dispersion.

Overall, very little is known about the global properties of the RR Lyrae stars in M31. The *HST* data available only cover a tiny fraction of its body, and they are all concentrated in the inner halo (Ferguson and Mackey, 2016). Moreover, as many satellite objects (such as NGC 205, the GSS, or And I) are embedded in, or projected along the line of sight, it is often difficult to unequivocally distinguish variables associated with either M31 or its satellite galaxies.

5.3 Isolated Dwarfs

At present, few Local Group galaxies are really isolated and located outside the virial radii of either the Milky Way or M31 (McConnachie, 2012). Nevertheless, a handful (DDO 210, VV 124, Sagittarius dwarf irregular galaxy) are truly iso-

lated systems in the sense that they are currently on their first approach of the innermost region of the Local Group, and they never experienced any strong interactions with either the Milky Way or M31. For some other galaxies, the situation is not as clear, because they are currently located outside the tidal radius of either major spiral galaxy, but we cannot exclude the possibility of past interactions (Fraternali et al., 2009). Detailed color–magnitude analysis reaching the old main-sequence turn-off of relatively and truly isolated Local Group dwarf galaxies requires use of the *HST*. The first systematic investigation of a representative sample of such galaxies has been performed by the LCID (Local Cosmology from Isolated Dwarfs) team (Gallart et al., 2015). Recently, more data have been acquired for DDO 210 (Cole et al., 2014), WLM, and Pegasus dwarf irregular (dIrr) galaxy (as yet unpublished). Studies of variable stars have been published by Bernard et al. (2009, Cetus and Tucana), Bernard et al. (2010, IC 1613), Bernard et al. (2013, Leo A), Clementini et al. (2012, Leo T), Ordoñez et al. (2014, Phoenix), and Ordoñez and Sarajedini (2016, DDO 210).

5.3.1 Purely old systems: *Cetus* and *Tucana*

Cetus and Tucana represent remarkable examples of isolated dwarf spheroidal (dSph) galaxies, since they are the only two gas-poor, purely old systems that do not follow the so-called density–morphology relation. In fact, the general tendency is that dSph systems are more clustered around large spirals, while dIrr galaxies are usually found in more isolated environments. However, Cetus and Tucana are the only two known purely old dwarf galaxies located at many hundreds of kpc from both the Milky Way and M31 (Monelli et al., 2010b). Nevertheless, their recessional velocities suggest that they may have been involved in an interaction a few Gyr ago (Sales et al., 2007; D’Onghia et al., 2009). Bernard et al. (2009) analyzed the detailed properties of RR Lyrae stars in both systems. Distance moduli were homogeneously derived by means of the LMR relation based on the Clementini et al. (2003) calibration and the FOBE method.

Despite many similarities among the general properties of their stellar populations, their star-formation histories (SFHs) were different during the oldest epochs. In particular, although the initial epoch of star formation was the same, the peak of the star-formation activity occurred at an earlier epoch in Tucana than in Cetus (Monelli et al., 2010a). This apparently subtle difference clearly emerges from the properties of their RR Lyrae stars. On the one hand, Monelli et al. (2012) presented a sample of more than 600 RR Lyrae stars in Cetus using wide-field Very Large Telescope (VLT)/VIMOS data and concluded that the properties of the RR Lyrae stars in Cetus are homogeneous over the entire galaxy body. The mean period, magnitude, and amplitude of the RR Lyrae stars do not significantly change as a function of radius, and overall, RR Lyrae stars seem to originate from a stellar population with similar chemical properties.

On the other hand, Tucana represents a much more complex case. Bernard et al. (2008) discussed the complex properties of a few hundred RR Lyrae stars, showing that the samples of bright and faint RR Lyrae stars have different pulsation properties and spatial distributions: faint stars are more centrally concentrated and their periods are shorter, at fixed amplitude. These results can be explained naturally if RR Lyrae stars exhibit an intrinsic spread in their metallicity distribution: faint RR Lyrae stars belong to a slightly more metal-rich population, consistent with them being preferentially formed in the innermost region of the galaxy, as commonly found in most nearby dSph galaxies.

These two examples strongly suggest that the detailed properties of RR Lyrae stars must be well-known in order to safely use them as distance indicators. If the population of RR Lyrae stars presents an intrinsic spread in metallicity (e.g., IC 1613, Bernard et al. 2010; Sculptor, Martínez-Vázquez et al. 2015; NGC 185, Monelli et al. submitted), it is risky to blindly adopt a mean luminosity and a mean metallicity for the entire sample. Bernard et al. (2009) derived the distance modulus of Tucana using the bright and the faint samples of RR Lyrae stars separately, assuming an appropriate metallicity constraint resulting from their SFH calculation, and they obtained consistent distance moduli, within the uncertainties.

5.3.2 Galaxies with extended SFHs

1. **IC 1613 and Leo A:** Whenever the SFH of a galaxy covers the full cosmic time, it is possible to use both old RR Lyrae stars and young classical Cepheids (CCs) to simultaneously obtain distance estimates. Examples of such analyses have been presented for IC 1613 (Bernard et al., 2010) and Leo A (Bernard et al., 2013). These authors used consistent assumptions and five different relations to derive their distance moduli, including period–luminosity and period–luminosity–color relations for CCs, combined with the LMR and FOBE methods for the RR Lyrae stars. Interestingly, while good agreement was found for IC 1613, the distance derived based on CCs was somewhat longer than that derived from RR Lyrae stars. In addition, a number of issues should be taken into account in assessing similar analyses. The periods of Cepheids can span from a few to hundreds of days. Therefore, it is very difficult, from an observational point of view, to collect a data set which allows for a good characterization of the light curves over the full period range, especially using *HST*. Nevertheless, coupling extensive ground-based data sets with dedicated and optimized space-borne observations has provided an excellent basis for such investigations. Scowcroft et al. (2013) provided a multiwavelength view of Cepheids in IC 1613, combining optical results from the OGLE survey (Udalski et al., 2001) with multi-epoch observations in JHK_s , obtained with the Magellan telescope, and at longer wavelengths using the *Spitzer Space Telescope*. The well-characterized optical light curves allowed them to detect and constrain the infrared properties of a Cepheid sample in IC

1613 and derive PLRs. The inclusion of deep *HST*/WFC3 near-infrared data allowed Hatt et al. (2017) to extend the comparison to RR Lyrae stars. These latter authors obtained very good agreement between Population I and Population II distance indicators. The same approach was used by Rich et al. (2014) to study the Cepheid population of NGC 6822. Combining optical OGLE detections with ground-based near-infrared and *Spitzer* mid-infrared data, Rich et al. (2014) derived six PLRs, as well as self-consistent distance and reddening estimates.

2. **DDO 210 and Phoenix:** DDO 210 is a low-mass, isolated galaxy with properties similar to those of Leo A (Cole et al., 2014). Its variable-star content has been studied by Ordoñez and Sarajedini (2016), who derived a distance modulus using the period–luminosity–metallicity relation in the *I* band of Catelan et al. (2004), once they had derived individual metallicities using the Alcock et al. (2000) relation.

Gallart et al. (2004) presented a large number of candidate RR Lyrae stars in Phoenix, but the data were not good enough for a detailed analysis. Such an analysis was, however, performed using *HST*/WFPC2 images by Ordoñez et al. (2014), who used RR Lyrae stars to study the early chemical evolution of Phoenix. Unfortunately, neither paper used RR Lyrae stars to derive distances.

Cepheids have been identified in both galaxies. However, the identification of CCs, especially in the short-period tail of the distribution, can be complicated by the presence of anomalous Cepheids (ACs). ACs and CCs both cross the instability strip during the central helium-burning phase of their evolution. The key difference with CCs is that ACs ignite helium in a degenerate core, while CCs are sufficiently massive that this occurs under non-degenerate conditions. Therefore, ACs have masses $\lesssim 2.3M_{\odot}$ and low metallicities ($[\text{Fe}/\text{H}] \lesssim -1.5$ dex; Fiorentino et al. 2006), since in this mass range, stars with higher metallicity evolve on the red side of the instability strip. Phoenix was the first system where CCs and ACs were found to coexist (Gallart et al., 2004). The coexistence of the two types of Cepheids has since been confirmed in other low-metallicity systems, including IC 1613 (Bernard et al., 2010), Leo A (Bernard et al., 2013), Leo I (Fiorentino et al., 2012b), and DDO 210 (Ordoñez and Sarajedini, 2016). Also, both Magellanic Clouds contain a small sample of ACs (Soszyński et al., 2008, 2016).

5.3.3 Leo T

Leo T is an intriguing low-mass, star-forming, relatively isolated dwarf galaxy. Using *HST*/WFPC2 data, Clementini et al. (2012) detected one RR Lyrae star and 12 ACs. This is because of the combination of its small total baryonic mass and its SFH, which is characterized by a dominant episode at intermediate ages and a low rate at early epochs. Nevertheless, the properties of the only RR Lyrae star discovered allowed an estimate of the distance modu-

lus, based on the Clementini et al. (2003) LMR, adopting a proxy metallicity, spectroscopically derived for the galaxy’s RGB stars.

5.4 RR Lyrae beyond the Local Group

The *HST* has allowed the discovery of RR Lyrae stars in a handful of dwarf galaxies outside the Local Group. Da Costa et al. (2010) first reported detections of RR Lyrae in two dwarf galaxies in the Sculptor group. Variables were later analyzed in detail by Yang et al. (2014). Individual metallicities were derived using the Alcock et al. (2000) method, and the mean metallicity of the distribution was used with the Chaboyer (1999) LMR relation. The derived distances, close to 2 Mpc, are in agreement, within the uncertainties, with other estimates based on the TRGB.

The only other galaxy external to the Local Group where RR Lyrae have been discovered is Leo P (McQuinn et al., 2015). This is a very interesting low-mass, gas-rich galaxy with an extended SFH, similar to Leo T. A distance modulus based on the 10 RR Lyrae discovered was obtained using the Carretta et al. (2000) LMR relation. The metallicity pertaining to the RR Lyrae stars was estimated by comparing the distribution of stars in the color–magnitude diagram with theoretical isochrones.

6 Toward homogeneous RR Lyrae-based distance determinations

6.1 The ISLAndS project

ISLAndS is an ongoing project targeting six M31 satellites with as main aim to compare the SFHs in the Milky Way and the M31 systems (Weisz et al., 2014; Monelli et al., 2016; Skillman et al., 2017). Full analysis of the variable stars will be presented in a series of forthcoming papers (Martínez-Vázquez et al., in prep). Key results regarding distance estimates are summarized here. The sample of galaxies includes And I, And II, And III, And XV, And XVI, and And XXVIII, thus spanning a wide range in mass, luminosity, and distance from M31. Next, we will use the ISLAndS galaxies as test cases to compare the performance of four different methods to derive their distance moduli. Three of the methods are based on the properties of the RR Lyrae stars, including (i) the reddening-free PWR (Marconi et al., 2015), (ii) the LMR (Bono et al., 2003; Clementini et al., 2003), and (iii) the FOBE relation (Caputo et al., 2000); these are supplemented by (iv) the TRGB method.

As a first step, the metallicity values were homogenized to Carretta et al. (2009) scale. For those galaxies with metallicity estimates based on theoretical spectra, we applied a correction to take into account the updated solar iron abundance, rescaling to $\log \epsilon_{\text{Fe}} = 7.54$ dex.

The second step is meant to ensure homogeneous assumptions for the metallicity. The metallicity estimates available in the literature were derived

using calcium-triplet spectroscopy of bright RGB stars. The mean metallicity of the RGB stars in And III (Kalirai et al., 2010), And XV (Letarte et al., 2009), And XVI (Collins et al., 2015), and And XXVIII (Slater et al., 2015), is close to $[\text{Fe}/\text{H}] \sim -1.8$ dex (or less). In agreement with the limited age and metallicity spreads characteristic of the dominant population, derived from the SFHs (Skillman et al., 2017), we assume that the spectroscopic mean metallicity is representative of the old population as well.

However, And I and And II exhibit higher mean metallicities and larger metallicity spreads (Ho et al., 2012, 2015). Nevertheless, the small number of high-amplitude, short-period (fundamental-mode) RRab-type stars in these galaxies (Fiorentino et al., 2015) suggests that, even if the tail of the RR Lyrae metallicity distribution reaches such relatively high values, the bulk of the RR Lyrae stars must have a lower metallicity ($[\text{Fe}/\text{H}] < -1.5$ dex; Fiorentino et al. 2015). Therefore, we adopted $[\text{Fe}/\text{H}] = -1.8$ dex as representative of the mean metallicity of the RR Lyrae stars in And I and And II.

Once the metallicity had been fixed, we estimated the distance moduli to the ISLAndS galaxies as outlined below. The results are summarized in Fig. 2 and Table 3.

1. **Period–Wesenheit relations:** Since the data were originally calibrated according to the VEGAMAG system, individual phase points were recalibrated to the Johnson system using the transformation provided by Bernard et al. (2009) and optimized for the RR Lyrae color range. Since the F475W filter is characterized by a wide passband, similar to the g band, measurements were calibrated in both the B and the V filters, while the F814W band was transformed to the Johnson–Cousins I filter. This allowed us to use two PWRs from Marconi et al. (2015), the $(I, B - I)$ and $(I, V - I)$ relations, but not the metallicity-independent $(V, B - V)$ PWR, because the B and V measurements are not independent. For the adopted relations, a metallicity dependence is present, but it is weak: a change of 0.3 dex translates into a change in the distance modulus of order 0.03 mag. We applied both relations to the samples of RRab- and RRC-type variables, as well as to the total sample (RRab + fundamentalized RRC: $\log P_{\text{fund}} = \log P_{\text{RRC}} + 0.127$; Bono et al. 2001). The comparison shows very good agreement among the different determinations, on average within ± 0.04 mag. Since the number of stars in the full sample is the largest, we selected as final adopted distance modulus the mean value of the distance moduli calculated using both PWRs and that for the full sample. Table 3 presents for the six galaxies (Col. 1) the range of distance moduli available in the literature (Col. 2), and our final estimate based on the PWR of the full sample of RR Lyrae stars (Col. 3).
2. **Luminosity–metallicity relation:** We adopted two different relations, i.e., those proposed by Clementini et al. (2003) and Bono et al. (2003). The zero-point of the former was modified such that the distance modulus to the LMC is in agreement with the distance modulus obtained by Pietrzyński et al. (2013), assuming $[\text{Fe}/\text{H}] = -1.5$ dex for the RR Lyrae

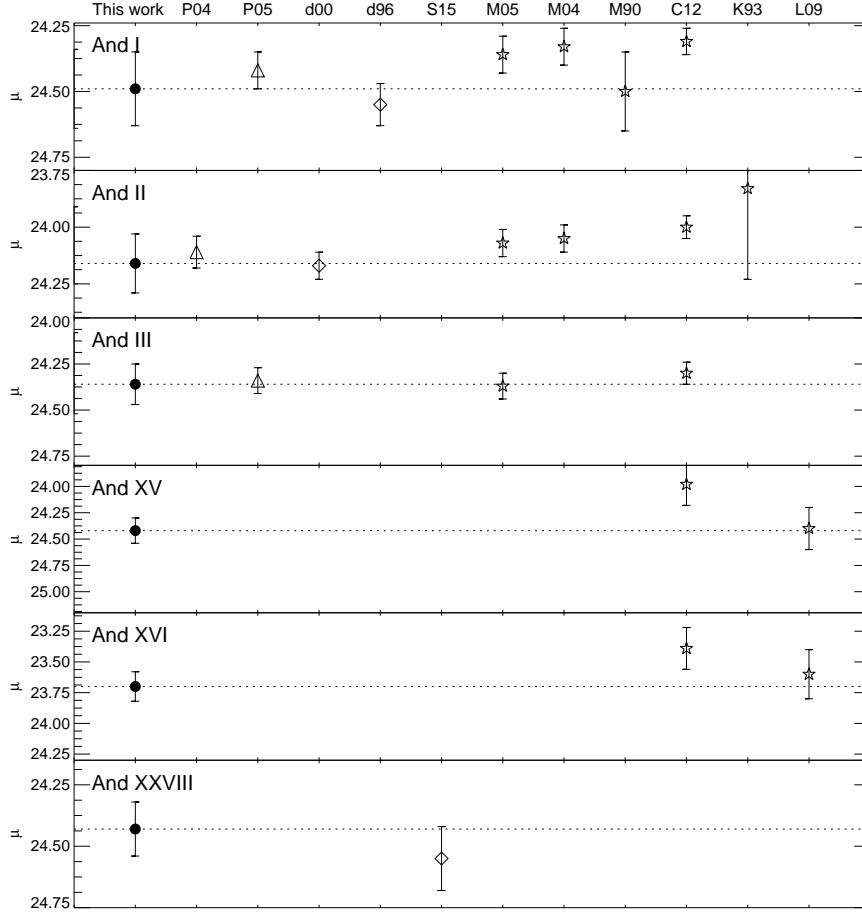


Fig. 2 Summary of our distance modulus estimates (solid symbols) and comparison with literature values (open symbols). Estimates based on the TRGB are provided only for the most massive galaxies, for which the TRGB could be estimated reliably. The solid circles and dotted lines show the measurements based on the PWR relations. Other symbols show values taken from the literature, for comparison. In particular, we report values based on RR Lyrae stars (asterisks: Pritzl et al., 2002a, 2005a), the HB luminosity (open squares: Da Costa et al., 1996, 2000; Slater et al., 2015), and the TRGB (open diamonds: Mould and Kristian, 1990; Koenig et al., 1993; McConnachie et al., 2004, 2005; Conn et al., 2012).

stars (Gratton et al., 2004). The resulting equation is therefore

$$M_{V,C03} = 0.892 \pm 0.052 + (0.214 \pm 0.047)[\text{Fe}/\text{H}]. \quad (1)$$

The second calibration adopted was a double-linear relation with a break in the slope at $[\text{Fe}/\text{H}] = -1.6$ dex. We adopted the lower metallicity, appropriate for the six ISLAndS galaxies ($[\text{Fe}/\text{H}] = -1.8$ or less).

Galaxy	True distance moduli	
	Literature value (mag)	PWR (mag)
And I	24.31–24.55	24.51±0.08
And II	23.87–24.17	24.17±0.07
And III	24.30–24.37	24.38±0.06
And XV	23.98–24.4	24.43±0.07
And XVI	23.39–23.6	23.71±0.07
And XXVIII	24.55±0.13	24.45±0.05

3. **The FOBE method:** This method is based on the predicted period–luminosity–metallicity relation for pulsators located along the FOBE of the instability strip (see Caputo et al., 2000):

$$M_{V,\text{FOBE}} = -0.685 - 2.255 \log(P_{\text{FOBE}}) - 1.259 \log(M/M_{\odot}) + 0.058 \log(Z). \quad (2)$$

This is a well-defined technique for stellar systems with a large number of RRc-type stars, in particular if the blue side of the first-overtone instability strip is well-populated. For this reason, we applied it only to five of our six galaxies, since the small number of RRc stars in And XVI may yield inconsistent results (Monelli et al., 2016). To derive the stellar masses, we adopted the BaSTI evolutionary models (Pietrinferni et al., 2004). For the selected metallicity, a star with an effective temperature typical of RRc stars ($\log T_{\text{eff}} \approx 3.86$ [K]), we derived values of $M \sim 0.7M_{\odot}$. Distance moduli obtained for each galaxy using this method are included in Fig. 2.

4. **Tip of the RGB:** The TRGB is a well-studied, work-horse standard candle by virtue of its weak dependence on both age (Salaris and Weiss, 2002) and, particularly in the *I* band, on the metallicity (at least for relatively metal-poor systems; Da Costa and Armandroff, 1990; Lee et al., 1993). The TRGB is frequently used to obtain distance estimates to galaxies of all morphological types (e.g., Rizzi et al., 2007; Bellazzini et al., 2011; Wu et al., 2014). However, determining the cut-off in the luminosity function at the bright end of the RGB is not straightforward in low-mass systems because of the inherently small number of bright RGB stars (Madore and Freedman, 1995; Bellazzini et al., 2001, 2008). A total of more than about 100 stars in the top magnitude range of the RGB is considered a safe threshold for reliable estimates. In our galaxies, this condition is met only by And I ($N > 200$), And II ($N > 150$), and nearly in And III ($N \sim 90$). The small numbers of such stars in the other three galaxies prevent us from deriving reliable measurements of the apparent magnitudes of their TRGBs. We adopted the calibrations of Rizzi et al. (2007), Bellazzini et al. (2011) and Cassisi and Salaris (2013) to compile Fig. 2.

Figure 2 summarizes the distance modulus determinations derived in this paper. In particular, the solid circles and the dotted line show the adopted

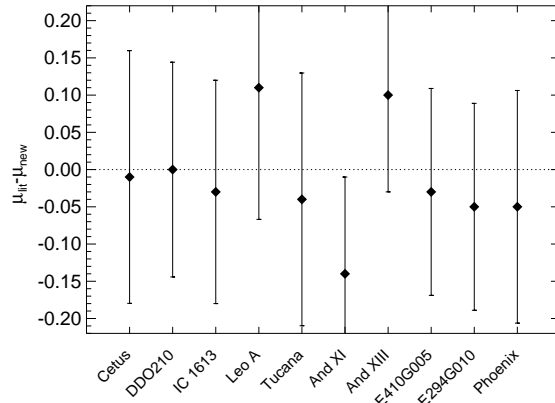


Fig. 3 Differences between distance-modulus estimates obtained based on RR Lyrae stars and literature values for a number of galaxies. These updated values represent homogenized metallicities, employing the Marconi et al. (2015) PWR.

final distance moduli based on averaging the values from the two PWRs. Filled diamonds show the results from the other methods. This figure shows that the agreement among the different methods employed here is remarkably good, since most of the derived distance moduli agree within 1σ . Taking as reference the PWR distance, some general trends can be discerned. The distance derived using the LMR based on the Bono et al. (2003) calibration is marginally longer with respect to that resulting from the Clementini et al. (2003) calibration. The FOBE distance is longer than the PWR distance in three cases (And III, And XV, and And XVI) and shorter for And II. Nevertheless, this method is most sensitive to the sampling of the instability strip, and in particular the lack of RR Lyrae close to the blue edge of the instability strip introduces a bias toward greater distances.

Asterisks and open symbols in Fig. 2 represent distance modulus estimates available in the literature, derived using different techniques, including those based on RR Lyrae stars (asterisks: Pritzl et al., 2002b, 2005b), the HB luminosity (open squares: Da Costa et al., 1996, 2000; Slater et al., 2015), and the TRGB (open diamonds: Mould and Kristian, 1990; Koenig et al., 1993; McConnachie et al., 2004, 2005; Conn et al., 2012). Figure 2 shows generally good agreement with our estimates, within the uncertainties. Note that the TRGB tends to yield shorter distances than the RR Lyrae and the HB luminosity-based methods, although they are still compatible within 1.5σ . A number of discrepant cases (And XV and And XVI; see Conn et al. 2012) can be ascribed to the sparsely populated bright part of the RGB in these galaxies.

Galaxy	Distance moduli		
	Literature (mag)	PWR (mag)	LMR (mag)
Cetus	24.46±0.12 ^a	24.47±0.02±0.04	24.43±0.08
DDO 210	25.07±0.12 ^b	25.07±0.03±0.05	—
IC 1613	24.44±0.09 ^c	24.47±0.02±0.04	23.41±0.08
Leo A	24.57±0.13 ^d	24.46±0.07±0.10	24.41±0.08
Tucana	24.74±0.12 ^e	24.78±0.01±0.05	24.72±0.08
And XI	24.33±0.05 ^f	24.47±0.05±0.16	24.55±0.08
And XIII	24.62±0.05 ^g	24.52±0.07±0.14	24.72±0.08
ESO410-G005	26.33±0.07 ^h	26.36±0.01±0.23	26.36±0.08
ESO294-G010	26.40±0.07 ⁱ	26.45±0.01±0.20	26.42±0.08
Phoenix	23.09±0.10 ^j	23.14±0.02±0.15	23.17±0.08

^aBernard et al. (2009), ^bOrdoñez and Sarajedini (2015), ^cBernard et al. (2013), ^dBernard et al. (2013), ^eBernard et al. (2009), ^fYang and Sarajedini (2012), ^gYang and Sarajedini (2012), ^hYang et al. (2014), ⁱYang et al. (2014), ^jHidalgo et al. (2009).

6.2 Revising the distances to Local Group galaxies

Using existing data to construct a homogeneous distance framework for a large number of Local Group galaxies is still far from having been achieved. Ideally, one would want to derive homogeneous pulsation properties and metallicities, and then uniformly use RR Lyrae stars to derive distances. However, the highly inhomogeneous data set available (in terms of data quality, filter passbands used, and completeness) renders this a complicated task. Moreover, different authors often use different methods of data analysis and, critical in this case, different approaches and assumptions as regards the metallicity.

In an incomplete attempt to resolve this situation, based on a similar approach as that adopted for the ISLANDS sample, we re-analyzed the available data for a sample of Local Group galaxies for which high-quality *HST* data are available. This includes galaxies characterized by different levels of isolation and extends to systems in the Sculptor group. We selected those galaxies for which photometry in the Johnson *V* and *I* or in the *B* and *I* bands is available in the literature.¹ We assumed a metallicity of $[\text{Fe}/\text{H}] = -1.8$ dex as representative of the RR Lyrae stars in all galaxies.

New distances were derived using the $(I, V - I)$ PWR, with the exception of DDO 210, for which only *B* and *I* catalogs are available. A second estimate was obtained using the LMR, based on the Clementini et al. (2003) calibration and updated as described in the previous section. Table 6.2 summarizes the results. Column 2 presents the original literature values; we included only estimates based on RR Lyrae stars, with the exception of Phoenix (Hidalgo et al., 2009;

¹ We emphasize that we did not attempt to use the original photometry in the VEGA-MAG system and transform it, since the original data are often not provided. Therefore, the photometric conversion to the Johnson system may have been performed using different methods by different authors. Although we do not expect this to introduce significant systematics in the distance determination, this issue must be taken into account for future investigations.

Ordoñez et al., 2014). Columns 3 and 4 present the same distance estimates recalculated using the PWR and the updated LMR (Eq. 1). Both methods show excellent agreement in most cases. Figure 3 shows the differences between the literature values and our updated values based on the PWR. Note that, overall, the literature values are based on slightly higher mean metallicities than adopted for our recalibration ($[\text{Fe}/\text{H}] = -1.5$ dex for Leo A, values between $[\text{Fe}/\text{H}] = -1.6$ and -1.8 dex for the other galaxies). This can account for up to few hundredths of a magnitude in distance differences. Nevertheless, the change is small, at the level of at most $\sim 1\sigma$, where the error bars reflect realistic estimates of systematic and random uncertainties associated with the method.

7 Internally consistent distance determination beyond the nearest galaxies

Internally consistent determinations of the Hubble constant well beyond the Local Group, based on cross-correlation of a variety of independent techniques, are crucially important for establishing the three-dimensional morphology of the Universe on the largest scales. By association, such measurements provide indirect tests of the consistency of the cosmological framework implied by SNe Ia measurements. Distance measurements at these distances are particularly important in the context of reducing the effects of galaxies' peculiar velocities as well as regarding the inhomogeneity of the matter distribution, which is the root cause of the difference between the locally measured and the true, global values of the Hubble constant (e.g., Turner et al., 1992).

SNe Ia are bright standard candles and, hence, in principle they enable distance measurements out to cosmological scales ($z \sim 1$). However, to use SNe Ia as absolute distance indicators, their absolute magnitudes must be calibrated using carefully selected primary distance indicators such as Cepheid variables (e.g., Riess et al., 2016). To check for the possible effects of unknown systematics, those distances should be compared with a set of independent distance measurements that do not rely on mutually dependent calibrations of the distance ladder. Megamasers can be used to directly measure distances to galaxies out to ~ 50 Mpc, which is sufficiently distant to reduce the effects of peculiar velocities (Reid et al., 2009). Here, we review several other independent techniques that may potentially serve as important tests of the absolute distance scale beyond the nearest galaxies.

7.1 Clusters of galaxies

Combined with X-ray data, observations of the Sunyaev–Zel'dovich effect (SZE) affecting massive clusters of galaxies can be used to infer the Hubble constant (Silk and White, 1978). This is because the X-ray surface brightness depends on $S_X \propto \int n_e^2 A d\ell$, where A is the X-ray cooling function determined

from the gas temperature T_e , and the SZE depends on $y \propto \int n_e T_e d\ell$. Assuming spherically shaped galaxy clusters, line-of-sight distances can be expressed as $d\ell \sim D_A d\theta$, where D_A is the angular diameter distance and θ the cluster's angular size. By eliminating the electron density, n_e , the angular diameter distance can be expressed in terms of X-ray and SZ observables as $D_A \propto y^2/S_X$, assuming spherical symmetry. The effects of non-spherical cluster morphologies can be reduced by averaging H_0 measurements for many clusters.

Reese et al. (2002) determined distances to 18 clusters at $z = 0.14 - 0.78$ to constrain the Hubble constant to $H_0 = 60_{-3}^{+4}(\text{statistical})_{-18}^{+13}(\text{systematic}) \text{ km s}^{-1} \text{ Mpc}^{-1}$. Bonamente et al. (2006) obtained an updated result, $H_0 = 76.9_{-3.4}^{+3.9}(\text{stat.})_{-8.0}^{+10.0}(\text{syst.}) \text{ km s}^{-1} \text{ Mpc}^{-1}$ using 38 clusters at $z = 0.14 - 0.89$. These analyses suggest that the dominant uncertainty affecting this method is already determined by various systematic errors, such as inhomogeneities in the intracluster medium (e.g., Kawahara et al., 2008). This may imply that a better understanding of the physical state of the intracluster medium (e.g., Hitomi Collaboration, 2016) is crucial to obtain more accurate distance measurements based on this approach.

7.2 Relative ages of old galaxies

Jimenez and Loeb (2002) proposed to use relative ages of passively evolving galaxies at a range of redshifts to directly constrain the Hubble parameter, $H(z)$. Spectra of passively evolving galaxies are dominated by main-sequence stars of $M \sim 1M_\odot$, for which the relevant stellar evolution processes are well-understood. In addition, relative ages can be determined more easily and with higher accuracy than absolute ages, because several systematic effects are factored out. Once the relative ages at different redshifts have been determined, one can derive the Hubble parameter by employing the relation $H(z) = -(dz/dt)/(1+z)$. Jimenez et al. (2003) applied this technique to Sloan Digital Sky Survey (SDSS) galaxies at $z < 0.17$ to obtain $H_0 = 69 \pm 12 \text{ km s}^{-1} \text{ Mpc}^{-1}$, which is consistent with other H_0 measurements. Further theoretical and observational studies aimed at improving our understanding of galaxy spectra have the potential to reduce the remaining uncertainties in the current-best values of H_0 .

7.3 Gravitational waves as standard sirens

Gravitational waves from inspiraling compact binaries are well placed to become useful as absolute distance indicators (Schutz, 1986; Holz and Hughes, 2005). They are sometimes referred as ‘standard sirens.’ This is because masses of inspiraling and merging objects, such as neutron stars and black holes, can be inferred from the shape of the waveform (e.g., from the frequency and its time evolution), which also determines the absolute strain amplitude (a dimensionless parameter that depends on the strength of the tidal gravitational

field between both binary components). We can then directly measure the luminosity distance to a gravitational-wave source, because the observed strain is inversely proportional to the luminosity distance.

We can measure luminosity distances using gravitational-wave standard sirens, but not the associated redshifts. Therefore, independent observations of the objects' electromagnetic counterparts are usually required to locate the host galaxy of a gravitational-wave event and measure its redshift to constrain the Hubble constant. For instance, Dalal et al. (2006) discussed the possibility of simultaneous observations of short gamma-ray bursts and gravitational waves from merging neutron-star binaries. They argued that several tens of such observations can constrain the Hubble constant to the $\sim 2\%$ level.

A major advantage of this method is its 'clean' physics. Assuming that general relativity is valid, the waveforms of such merging events can be computed easily from first principles. On the other hand, obtaining observations of gravitational waves has been a significant challenge for decades. Recently, the first observation of gravitational waves, referred to as GW150914, from a pair of black holes has been reported (Abbott et al., 2016). This has now finally opened up the possibility of using gravitational waves as a tool to benchmark the cosmic distance scale. Whereas it is not yet clear whether binary black hole mergers produce any detectable electromagnetic counterparts for redshift measurements, it may also be possible to use the spatial cross-correlation of gravitational-wave sources and galaxies with known redshifts to constrain the Hubble constant without any observations of electromagnetic counterparts (Oguri, 2016). For this cross-correlation technique to become viable, we need observations of large numbers of gravitational waves over the entire sky, as well as decent localizations of gravitational-wave sources, with an accuracy of $\sim 1^\circ$. This will become possible with the next-generation of gravitational-wave detectors.

8 Gravitational lensing as a promising tool

Time delays of strongly lensed quasars provide a one-step measurement of a cosmological distance, namely the time-delay distance to the lens system (e.g., Refsdal, 1964; Suyu et al., 2010). With additional information from the stellar velocity dispersion of the lens, we can further constrain the associated angular diameter distance (Paraficz and Hjorth, 2009; Jee et al., 2015). In a companion review, we have described the recent cosmological constraints based on this approach, particularly those based on the COSMOGRAIL (Courbin et al., 2005, 2011; Eigenbrod et al., 2005; Tewes et al., 2013) and H0LiCOW (Sluse et al., 2016; Bonvin et al., 2017; Rusu et al., 2017; Suyu et al., 2017; Wong et al., 2017) projects. Here, we describe the future prospects for this approach, focusing in particular on (i) expanding the time-delay lens sample and (ii) follow-up observations, in light of upcoming missions and surveys.

8.1 Where are the time-delay lenses?

Quadruply lensed quasars (‘quads’) with ancillary data can each provide a time-delay distance measurement of $\sim 5 - 8\%$. However, currently only a handful of quads are known at present. For example, there are only four quads in the H0LiCOW sample of lenses for cosmography (Suyu et al., 2017). There are several times more doubly lensed quasars (‘doubles’), but accurate and precise² distance measurements from these systems would be more challenging compared to the equivalent determinations based on quads, since doubles have fewer observational constraints compared with quads. For example, quad systems can yield four image positions and flux measurements of quasars as constraints, whereas double systems have half of that number as constraints. In addition, quads can have three time-delay measurements between the multiple images, which is substantially better for cosmographic studies than the single time-delay measurement available in doubles. Unless we can find more time-delay lenses, especially quads, the statistical power of this approach will be limited.

Fortunately, discoveries of hundreds if not thousands of time-delay lenses are expected in current and future surveys and missions, with $\sim 13\%$ of them being quads (Oguri and Marshall, 2010; Liao et al., 2015). Below, we describe three ongoing imaging surveys that will likely expand the current sample of quads by an order of magnitude:

1. **Dark Energy Survey (DES):** The DES (Dark Energy Survey Collaboration et al., 2016) uses the 4 meter Mayall telescope at Cerro Tololo observatory in Chile. Its large-format CCD array of 74 detectors covers, in one single snapshot, an area of 2.2 degrees on a side (Flaugher et al., 2015). After five years of operation the full survey will cover $\sim 5000 \text{ deg}^2$ in the g, r, i, z , and Y bands down to $r = 24.3 \text{ mag}$ (10σ). DES has already discovered lensed quasars. Two were reported in Agnello et al. (2015b) in the context of the SRIDES program (Agnello and Treu, 2015). In addition, a doubly imaged quasar (Ostrovski et al., 2017) was found in the data taken during the first year of the survey. Many more are found at the time of writing this review, as the data obtained during the second year are analyzed. Given the area and depth of the survey, Oguri and Marshall (2010) predicted that a total of ~ 1000 new lensed quasars should be found upon completion of the survey.
2. **Hyper Suprime-Cam (HSC) Survey:** The HSC survey is a Subaru Strategic Program, using the newly installed HSC (Miyazaki et al., 2012) on the Subaru 8.2 meter telescope, which is capable of imaging a large area of the sky in a single pointing³. The survey started in 2014 and is divided into three layers characterized by different areas and depths, i.e., wide, deep, and ultra-deep. In particular, we expect to find most of the

² Accuracy is a measure of how close the values are to the target or standard value; precision reflects their spread around the mean.

³ <http://hsc.mtk.nao.ac.jp/ssp/>

new lenses in the wide survey, which will cover $\sim 1400 \text{ deg}^2$, mostly in equatorial regions, to $i \sim 26$ mag in *grizy* broad bands with excellent seeing ($\sim 0.6''$ in the *i* band). The first-year HSC survey data covering over 100 deg^2 in the five broad bands have recently been released to the public (Aihara et al., 2017). The expected number of lensed quasars in the HSC survey is ~ 600 (Oguri and Marshall, 2010).

3. **Kilo-Degree Survey (KiDS):** The KiDS program is running at the European Southern Observatory’s Paranal observatory in Chile (Kuijken et al., 2015). It uses the 2.6 meter VLT Survey Telescope (VST) in the *ugri* optical bands and covers 10-degree wide strips, including an equatorial one between $10^{\text{h}}20^{\text{m}} < \text{RA} < 15^{\text{h}}50^{\text{m}}$ and a southern strip going through the Galactic South Pole, $12^{\text{h}}00^{\text{m}} < \text{RA} < 03^{\text{h}}30^{\text{m}}$. The total area covered is $\sim 1500 \text{ deg}^2$, i.e., similar to the HSC survey. The observing strategy is designed to ensure the best seeing in the *r* band, which has a median seeing of $\sim 0.7''$. The depth in this band is $r = 24.9$ mag (AB, 5σ). Overall, KiDS should be as efficient as HSC in finding bright, strongly lensed quasars.

Various new algorithms have been developed for finding galaxy-scale lenses, many of which have been applied to these imaging surveys. Here we focus on automated algorithms that are aimed at finding lensed quasars, although there are also methods to find lensed galaxies without quasars (e.g., Bolton et al., 2006; Gavazzi et al., 2014; Joseph et al., 2014; Napolitano et al., 2015; Paraficz et al., 2016; Shu et al., 2016; Sonnenfeld et al., 2017) or lens systems in general via visual inspection by citizen scientists (e.g., Marshall et al., 2016; More et al., 2016b). While most of the first lensed quasars were found at radio wavelengths through the Cosmic Lens All-Sky Survey (Myers et al., 2003), the SDSS has yielded dozens of lensed quasars through the SDSS Quasar Lens Search (e.g., Oguri et al., 2006; Kayo et al., 2010; Inada et al., 2012; Oguri et al., 2012) and, more recently, another 13 two-image lensed quasars (More et al., 2016a). The advantage of using SDSS is the availability of a spectroscopic quasar sample from which one could search for lensed objects. Consequently, lenses obtained from such a search will guaranteed be lensed quasars, rather than lensed galaxies (without quasars), which are more numerous than lensed quasars but not time-varying. Current imaging surveys such as HSC, DES, and KiDS do not include a spectroscopic component as part of the surveys. Therefore, recent searches necessarily rely on color information by selecting objects with colors and morphologies compatible with lensed active galactic nuclei (e.g., Jackson et al., 2012; Agnello et al., 2015a,b; Ostrovski et al., 2017; Schechter et al., 2017). In addition, as advocated by Marshall et al. (2009), for an object to qualify as a lens, it must have a physical lens mass model. This is the basis of the model-based search algorithms such as CHITAH (Chan et al., 2015) and LensTractor (Marshall et al., in prep.). Moreover, Kochanek et al. (2006) have proposed to use quasar variability to find lens systems by looking for clustered (possibly blended) variable sources corresponding to the multiple quasar images. Our expectation is that these surveys will each contain hun-

dreds to about a thousand lensed quasars (Oguri and Marshall, 2010), and efforts are underway to find these.

Two surveys planned for execution the 2020s should yield yet another order-of-magnitude increase in the number of lenses compared with current surveys:

1. **Euclid:** The first space-based, wide-field cosmological survey will be the ESA/NASA *Euclid* 1.2 meter telescope (Laureijs et al., 2011). Once placed at the L2 Sun–Earth Lagrange point in 2020, this satellite will be equipped with a 0.5×0.5 deg² optical imager, which uses a single broad filter covering the $R+I+Z$ bands, as well as a near-infrared imager covering the same field of view to perform imaging in the Y , J , and H bands. In total, *Euclid* will cover $\sim 15,000$ deg² of extragalactic sky down to a 10σ optical AB magnitude of 24.5 mag and down to a 5σ AB magnitude of 24.0 mag in each of the three near-infrared bands. An additional deep survey will include 40 deg² of sky two magnitudes deeper than the wide survey. *Euclid* will image a total of 12 billion sources (3σ) and it will obtain near-infrared slitless spectra of 35 million of these. With its excellent image quality and point-spread-function (PSF) stability, *Euclid* is optimized for weak-lensing tomography and it will also implement other cosmological probes such as baryon acoustic oscillations, the integrated Sachs–Wolfe effect, galaxy cluster counts, and redshift space distortions. With its sharp PSF ($0.18''$ FWHM), *Euclid* will also be a superb machine to discover gravitationally lensed quasars with an image quality that, on its own, already allows one to constrain lens models.
2. **Large Synoptic Survey Telescope (LSST)**⁴: The LSST is an ambitious new survey telescope that is under construction in Chile. The telescope has a primary mirror diameter of 8.4 meters, with an effective aperture of 6.7 meters (because of the tertiary mirror area in the middle of the primary–tertiary mirror and some obscuration). It will rapidly survey the entire visible southern sky of $\sim 20,000$ deg² twice each week, for 10 years. Each patch of sky it will be visited 1000 times during the survey, in six filters, *ugrizy*. The survey will reach 24.5 mag depth in a single visit (30 seconds) and 27.5 mag co-added depth. The four primary science objectives of the LSST that drive the survey design are (i) constraining dark energy and dark matter, (ii) taking an inventory of the solar system, (iii) exploring the transient optical sky, and (iv) mapping the Milky Way. LSST will be revolutionary in the area of gravitational lensing. Thousands of lensed quasars will be found by LSST (Oguri and Marshall, 2010), and at least hundreds of them will have well-defined time delays measurable directly from the survey data alone (Liao et al., 2015).

⁴ <https://www.lsst.org/>

8.2 Observational follow-up requirements and analysis

8.2.1 Confirmation

Both high angular-resolution images and spectroscopy would help reveal whether the lens candidates, found in ground-based imaging surveys, are gravitational lenses or other astrophysical systems.

With high-resolution images, one can check whether the multiple image features are consistent with lensing morphology. While *Euclid* images are of high-resolution by default, space-based or adaptive-optics ground-based images could be used to confirm candidates from ground-based imaging surveys. Nonetheless, some systems observed with high-resolution imaging could still be difficult to decipher, for example, a doubly-imaged quasar and a star-quasar-galaxy chance alignment could look similar in high-resolution images, in which case spectroscopy is needed for confirmation.

Identical spectra of multiple components/features of an object would confirm the object to be a strongly lensed system, with the multiple components originating from the same source. Spectroscopic confirmation could further yield spectroscopic redshift measurements of the lens and/or the source, which are crucial pieces of information to convert the angular quantities which we measure to physical quantities.

8.2.2 Follow-up observations

With ground-based and upcoming space-based wide-field surveys, not only does finding lensed quasars become a fairly easy task, but also some of the follow-up observations required to confirm (or not) the candidates come for free. KiDS, DES, LSST, and all deep, multi-band ground-based surveys have at least one of their bands optimized for weak-lensing measurements. As a consequence, measuring the colors of the individual quasar images can be done directly from the survey data. In many cases, detecting the lensing galaxy or galaxies among the quasar images is possible from the weak-lensing quality images. However, additional ingredients are necessary to use the confirmed lensed quasars for cosmological purposes.

1. **The lens redshift and velocity dispersion:** In the era of modern wide-field surveys, the survey data on their own offer the required material to deblend the lensed images of the quasar and fit a crude lens model. More difficult are measurements of the lens redshifts, since they are often hidden in the glare of the quasar images, so that this requires long exposure times on 10 meter class telescopes. In COSMOGRAIL, Eigenbrod et al. (2006, 2007) measured 15 lens redshifts based on 2 hour exposure times and slit spectroscopy with the VLT. To separate the spectra of the quasar images from that of the lens galaxy, the data are spatially deconvolved (Courbin et al., 2000) using the spatial information contained in the spectra of PSF stars, obtained in multi-slit mode. The same technique can

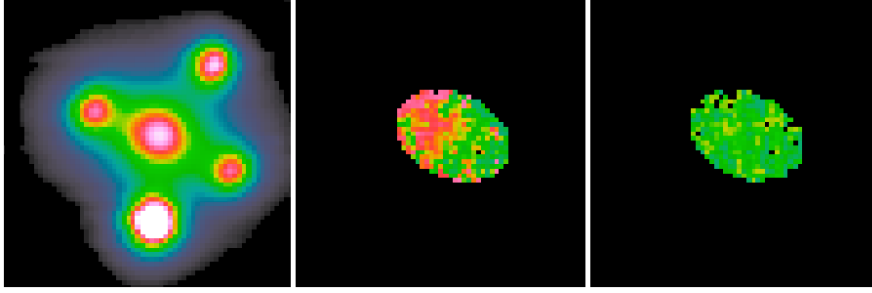


Fig. 4 (Left) Reconstructed image of the Einstein Cross, Q2237+080, seen with the near-infrared SINFONI integral-field spectrograph mounted on the VLT. The field of view is $3''$ on a side. North is up and East to the left. No adaptive optics was used to obtain this 6 hour integration with $0.5''$ seeing. (Middle) Radial-velocity field showing a small rotation signal. The maximum velocity in this $1''$ field is 60 km s^{-1} . (Right) Line-of-sight velocity-dispersion field, which is relatively flat with a mean value of $\sigma_r = 160 \pm 20 \text{ km s}^{-1}$ (From Eigenbrod 2009, PhD Thesis).

be used to measure the velocity dispersion of the lensing galaxy. This requires, however, longer exposure times and an instrumental setup with higher spectral resolution. With the advent of integral-field spectrographs, in combination with adaptive optics, or mounted on the *James Webb Space Telescope (JWST)*, it will become possible to map the full velocity fields and the velocity-dispersion fields of lens galaxies, hence providing a new wealth of observational constraints useful in breaking the degeneracies inherent to lens models. Figure 4 illustrates what is possible already with the near-infrared two-dimensional SINFONI spectrograph mounted on the VLT.

2. **High-resolution imaging of the lensed quasar host:** Quasar time delays depend on the slope of the lens mass at the position of the quasar images, which is the quantity we need to constrain with observations. One route to such a mass-slope measurement is use of the Einstein ring formed by the quasar host galaxy. If the latter is radially extended, the leverage on the mass slope of the lens is sufficiently good to fit simple lens models such as power-laws or more physically justified models involving stellar and dark matter components (Suyu et al., 2014, their Fig. 2). Fortunately, such rings are visible in most lensed quasars with time delays, provided that deep and high-resolution images can be taken, as in the H0LiCOW project (e.g. Suyu et al., 2017). Notably, the cosmological constraints derived using *HST* imaging can be further improved with Keck adaptive optics (Chen et al., 2016). *JWST* and the new generation of ground-based 30–40 meter-class telescopes have the potential to revolutionize the field thanks to the levels of detail achievable in the images of Einstein rings (Meng et al., 2015).
3. **Line-of-sight effect:** While the multiple images of lensed quasars are formed by individual galaxies, the details of the image configuration and the precise slope of the total potential well at the image positions depend on the contributions from all massive objects up to the quasar redshift.

Lens galaxies are often found in groups, i.e., they may share the dark matter halo of the group they belong to, in addition to their own halo. The contribution of the group to the total deflection field must be evaluated. If it is massive enough, deriving a mass map is possible from a weak-lensing analysis (e.g. Kneib et al., 2000). However, one must also account for the contribution of all other masses along the line of sight. Currently, this is done by comparing galaxy counts measured in the field of view of strongly lensed quasars (e.g. Fassnacht et al., 2011) with galaxy counts in cosmological simulations (Hilbert et al., 2007, 2009). Lines of sight are chosen in the simulations with the same *relative* galaxy density as in the observations and used to derive a probability distribution function for the mass density toward a given lensed quasar (Suyu et al., 2010; Greene et al., 2013; Suyu et al., 2013; Rusu et al., 2016). Other, more sophisticated methods (Collett et al., 2013; McCully et al., 2017) have the potential to reduce the uncertainty along the line of sight to that dominated by statistical errors only. All the above methods require multiband imaging to measure photometric redshifts and stellar masses. Ideally, multi-object spectroscopy is desirable to infer in detail the mass contributions from all galaxies in the immediate vicinity of the lens ($< 15''$), as done recently for HE 0435-1223 (Sluse et al., 2016).

4. **Time-delay measurements:** Large-scale sky surveys and discoveries of thousands of new lensed quasars potentially allow a drastic reduction in the random uncertainties affecting distance estimates using time delays. However, current time-delay measurements, e.g., based on COSMOGRAIL, need years of photometric monitoring. The reason for this is that the time-delay precision is limited by microlensing by stars in the lensing galaxy, which act as secondary lenses in each quasar image. As stars move along the line of sight to the quasar images, they affect the quasar images' apparent brightnesses. This results in a flickering of the lensed images on time-scales similar to those of the intrinsic quasar variations and with similar (or sometimes larger) amplitudes. Our ability to measure time delays therefore depends on our effectiveness in disentangling microlensing (different in each quasar image) from intrinsic quasar variations (identical in each quasar image). Obviously, it would be much easier to separate the microlensing variations from the intrinsic quasar variations if they were acting on different temporal time-scales. This is, in fact, possible! Quasars show variations on very short time-scales, much shorter than those typical of microlensing. The *Kepler* light curves of active galactic nuclei reveal that essentially all quasars exhibit variations on time-scales of a week or two (Mushotzky et al., 2011). Since microlensing is present on scales of a few years, the microlensing versus quasar variations can be separated in frequency, provided that the low-amplitude and fast intrinsic quasar variations can be detected and measured. Typical slow quasar variations over time-scales of months have amplitudes on the order of 0.5 mag, whereas faster, week-long variations usually only span a few mmag (r.m.s.). For this reason, the future of lens monitoring may reside in high signal-to-noise and

high-cadence monitoring, e.g., with daily observations of lenses with a 2–4 meter-class telescope. Such observations allow one to catch the quasar variations, almost insensitive to long time-scale microlensing. Time-delay measurements become possible in 1 or 2 years per object instead of 10–15 years, as is currently the case for smaller telescopes and a coarser temporal sampling of one or two epochs per week. However, given the signal-to-noise ratio needed (1000 per quasar image and per epoch), it will be difficult to monitor more than 20 lenses per night at any given telescope. In addition, measuring time delays longer than 90 days is not possible with this high-cadence mode over 1 or 2 years, since the time delay becomes comparable to the object’s visibility period. Long-term monitoring with large telescopes capable of following hundreds of lenses per night, like the LSST, is therefore the other complementary route to enable large numbers of precise and accurate time-delay measurements.

8.2.3 Analysis and lens modeling

Modeling the lens-mass distribution and accounting for the mass structure along the line of sight to the quasar source are crucial to convert time delays into distance measurements. Deep imaging which reveals the Einstein ring is important to precisely constrain the lens-mass distribution near the location of multiple images, where it matters for cosmography. While this has been done mostly in the optical/infrared with thousands of intensity pixels (e.g., Kochanek et al., 2001; Koopmans et al., 2003; Dye and Warren, 2005; Suyu et al., 2009, 2013; Fadely et al., 2010; Birrer et al., 2016; Wong et al., 2017), interferometric radio data have also been employed (e.g., Kochanek and Narayan, 1992; Ellithorpe et al., 1996; Wucknitz et al., 2004). The recent completion of the Atacama Large Millimeter/submillimeter Array (ALMA), which provides high-sensitivity and high angular-resolution imaging, opens up a new avenue for modeling the Einstein rings (e.g., Hezaveh et al., 2013; Bussmann et al., 2015; Rybak et al., 2015; Hezaveh et al., 2016).

To model the observed images, simultaneous determination of the source surface brightness and the lens-mass distributions is needed. Numerous modeling approaches have been developed over the past decade (e.g., Warren and Dye, 2003; Suyu et al., 2006; Barnabè and Koopmans, 2007; Jullo et al., 2007; Jullo and Kneib, 2009; Suyu et al., 2009; Vegetti and Koopmans, 2009; Suyu and Halkola, 2010; Oguri, 2010; Collett and Auger, 2014; Tagore and Keeton, 2014; Birrer et al., 2015; Nightingale and Dye, 2015; Rybak et al., 2015; Hezaveh et al., 2016; Tagore and Jackson, 2016), some of which have been used recently to measure distances to lensed quasars (e.g., Suyu et al., 2010, 2013, 2014; Birrer et al., 2016; Wong et al., 2017). In order to avoid confirmation bias, the cosmographic analysis of the H0LiCOW collaboration (Suyu et al., 2017) is blinded (Suyu et al., 2013; Bonvin et al., 2017; Wong et al., 2017). For cosmographic inference, each lens takes an expert modeler weeks of analysis owing to the high computational load caused by the large numbers of data points (image pixels) and parameters (dozens) involved. While parallel computing can reduce the computational time, frequent

manual input from the expert modeler is often required. Automating the full modeling procedure is challenging given the complexity of lens modeling, but it is worth pursuing in the era of hundreds/thousands of lenses.

To break lens-modeling degeneracies caused by the mass-sheet degeneracy and source-position transformation (Falco et al., 1985; Gorenstein et al., 1988; Schneider and Sluse, 2013, 2014; Xu et al., 2016), additional information such as the stellar kinematics of the lens galaxy is needed. However, most of the lens modeling software suites tend to make use of only the lensing information and incorporate the kinematic information separately. Barnabè and Koopmans (2007) and Barnabè et al. (2011) provide self-consistent modeling of three-dimensional axisymmetric lens-mass distributions, although the cosmological implications of such a modeling strategy are yet to be explored. We expect that two-dimensional kinematic maps of lens galaxies would provide complementary information to break lens-parameter degeneracies, especially for two-image systems. Future lens modeling would benefit from including such kinematic information. As a demonstration, Suyu et al. (2014) found a $\sim 4\%$ discrepancy in the time-delay distance measurements between different lens mass models of a strong lens system owing to lensing degeneracies. Incorporating an aperture-averaged velocity dispersion measurement partially breaks the lensing degeneracy and reduces the discrepancy to $\sim 1\%$. In addition, kinematic data are the key ingredient for measuring the angular diameter distance to the lens (Jee et al., 2015). This distance measurement substantially improves the cosmographic constraints from time-delay distances alone, making time-delay lenses an even more competitive cosmographic probe (Jee et al., 2016).

In terms of quantifying line-of-sight structures, current approaches for cosmography are based on relative galaxy counts around a strong lens compared with those of simulations. With sufficient photometric and spectroscopic information of the structures along the line of sight, one could (in principle) attempt a full light-cone reconstruction of the mass. Steps into this direction have been carried out by, e.g., Collett et al. (2013), McCully et al. (2014), and McCully et al. (2017). This has the potential of achieving more precise and accurate inferences about the external convergence.

9 Future outlook

The detailed narrative provided in this review should have impressed upon the reader that efforts to establish an internally consistent distance framework from the nearest galaxies to the highest redshifts are indeed coming together on all scales. Analysis, theoretical, and observational developments are indeed very promising, with significant improvements in both accuracy and precision anticipated in the next few years.

We are at the dawn of a new era for variability studies. Current and future surveys are about to yield an unprecedented amount of information on the variable stars populating the Local Group. The European Space Agency's *Gaia* mission will result in the discovery of thousands of new RR Lyrae stars

in the Milky Way halo, and it will nail down the thorny systematics affecting the calibration of the luminosity–metallicity relation.

Going to near-infrared and longer wavelengths may also enable us to reduce the uncertainties in the distances to Local Group galaxies. At present, 2–3% distance accuracy is already achievable for distance estimates to the LMC, which may soon be improved to $\sim 1\%$. For instance, the Carnegie Hubble Program, using data from the warm *Spitzer* mission, derived $(m - M)_0^{\text{LMC}} = 18.477 \pm 0.034$ mag (Freedman et al., 2012). Ripepi et al. (2012) used near-infrared *VISTA* observations to derive $(m - M)_0^{\text{LMC}} = 18.46 \pm 0.03$ mag, while Inno et al. (2013) found $(m - M)_0^{\text{LMC}} = 18.45 \pm 0.02$ (stat.) ± 0.10 (syst.) mag based on optical/near-infrared PLR analysis of a large sample of fundamental-mode LMC Cepheids. These distances are within the mutual uncertainties of the direct, geometric distance determination based on eclipsing binaries obtained by Pietrzyński et al. (2013). The most recent SMC distance determination, which is based on mid-infrared analysis of fundamental-mode Cepheids, yields $(m - M)_0^{\text{mid-IR}} = 18.96 \pm 0.01$ (stat.) ± 0.03 (syst.) mag (Scowcroft et al., 2016, see also Graczyk et al. 2014). Extant and upcoming data will soon allow a systematic characterization of variable stars, thus reducing error bars and fixing the first rungs of the distance ladder.

Water maser measurements, first applied to obtain a geometric distance to NGC 4258 (Herrnstein et al., 1999, see also Table 1), have since been extended to other nearby systems. Preliminary efforts to determine a water-maser-based distance to M33 have thus far resulted in $D_{\text{M33}} = 750 \pm 140 \pm 50$ kpc— $(m - M)_0^{\text{M33}} = 24.38_{-0.64}^{+0.49}$ mag (total uncertainty)—where the first uncertainty in the linear distance determination is related to uncertainties in the HI rotation model adopted and the second uncertainty comes from proper-motion measurements (cf. de Grijs, 2013).

The LSST will produce a flood of data that will allow us to discover a close-to-complete sample of RR Lyrae stars out to hundreds of kpc, mapping the Milky Way’s halo and its substructures. Moreover, the next generation of extremely large telescopes will push the discovery of RR Lyrae stars to few Mpc, and of classical Cepheids out to ~ 100 Mpc.

Very Long Baseline Interferometry will enable geometric distance determination out to more than 100 Mpc, including to NGC 4258, M33, UGC 3789, and NGC 6264. Combined with *a priori* information on a galaxy’s rotation curve and its inclination with respect to our line of sight, we can construct a slightly warped ‘tilted-ring’ model of the galaxy’s dynamical structure. This, in turn, allows correlation of the angular proper motion measurements with the rotational velocity information obtained in linear units and, thus, provides an independent distance measurement.

Simultaneously, the Megamaser Cosmology Project (e.g., Reid et al., 2009, 2013; Braatz et al., 2010) aims at using extragalactic maser sources to directly measure H_0 in the Hubble flow, which is clearly very challenging at distances beyond 100 Mpc. The project team’s preliminary results look promising, however: using NGC 6264 ($D = 144 \pm 19$ Mpc) as a benchmark, they find $H_0 = 68 \pm 9$ km s $^{-1}$ Mpc $^{-1}$ (Kuo et al., 2013), which is indeed very close

to the current best determinations of H_0 based on a variety of independent measures. This looks like a promising way forward to eventually construct an internally consistent distance ladder with well-defined uncertainties out to the Hubble flow (see also Thévenin et al., 2017).

With the newly discovered lenses expected from upcoming surveys, the anticipated observational follow-up, and analysis developments, we expect that measuring distances to a sample of ~ 50 lenses should be feasible within the next few years. Jee et al. (2016) showed that with a sample of 55 bright lenses from current and future imaging surveys, the resulting cosmological constraints will be highly complementary and competitive to other cosmological probes, including the cosmic microwave background, baryon acoustic oscillations, and SNe.

Acknowledgements This research was partially supported by the National Natural Science Foundation of China (NSFC; grants U1631102, 11373010, and 11633005 to R.d.G.), the Spanish Ministry of Economy and Competitiveness (MINECO; grant AYA2014-56795-P to M.M. and C.E.M.-V.), the Max Planck Society through the Max Planck Research Group (S.H.S.), and the Swiss National Science Foundation (SNSF; F.C.). We thank ISSI-BJ for hospitality and an engaging workshop. We also acknowledge both referees for their constructive reviews.

References

- B.P. Abbott, et al. (LIGO Scientific Collaboration and Virgo Collaboration), Observation of Gravitational Waves from a Binary Black Hole Merger. *Phys. Rev. Lett.* **116**, 061102 (2016). doi: 10.1103/PhysRevLett.116.061102
- A. Agnello, T. Treu, STRIDES: Galaxy Evolution over Cosmic Time from new samples of Gravitationally Lensed Quasars. *Int'l Astron. Union General Assembly* **29**, id. 2257367 (2015).
- A. Agnello, B.C. Kelly, T. Treu, P.J. Marshall, Data mining for gravitationally lensed quasars. *Mon. Not. R. Astron. Soc.* **448**, 1446–1462 (2015a). doi: 10.1093/mnras/stv037
- A. Agnello, T. Treu, F. Ostrovski, P.L. Schechter, E.J. Buckley-Geer, H. Lin, M.W. Auger, F. Courbin, C.D. Fassnacht, J. Frieman, N. Kuropatkin, P.J. Marshall, R.G. McMahon, G. Meylan, A. More, S.H. Suyu, C.E. Rusu, D. Finley, T. Abbott, F.B. Abdalla, S. Allam, J. Annis, M. Banerji, A. Benoit-Lévy, E. Bertin, D. Brooks, D.L. Burke, A.C. Rosell, M.C. Kind, J. Carretero, C.E. Cunha, C.B. D’Andrea, L.N. da Costa, S. Desai, H.T. Diehl, J.P. Dietrich, P. Doel, T.F. Eifler, J. Estrada, A.F. Neto, B. Flaugher, P. Fosalba, D.W. Gerdes, D. Gruen, G. Gutierrez, K. Honscheid, D.J. James, K. Kuehn, O. Lahav, M. Lima, M.A.G. Maia, M. March, J.L. Marshall, P. Martini, P. Melchior, C.J. Miller, R. Miquel, R.C. Nichol, R. Ogando, A.A. Plazas, K. Reil, A.K. Romer, A. Roodman, M. Sako, E. Sanchez, B. Santiago, V. Scarpine, M. Schubnell, I. Sevilla-Noarbe, R.C. Smith, M. Soares-Santos, F. Sobreira, E. Suchyta, M.E.C. Swanson, G. Tarle, J. Thaler, D. Tucker, A.R. Walker, R.H. Wechsler, Y. Zhang, Discovery of two gravita-

- tionally lensed quasars in the Dark Energy Survey. *Mon. Not. R. Astron. Soc.* **454**, 1260–1265 (2015b). doi: 10.1093/mnras/stv2171
- H. Aihara, R. Armstrong, S. Bickerton, et al., First Data Release of the Hyper Suprime-Cam Subaru Strategic Program. *Publ. Astron. Soc. Jpn*, submitted (arXiv:1702.08449) (2017).
- C. Alcock, R.A. Allsman, D.R. Alves, T.S. Axelrod, A. Basu, A.C. Becker, D.P. Bennett, K.H. Cook, A.J. Drake, K.C. Freeman, M. Geha, K. Griest, L. King, M.J. Lehner, S.L. Marshall, D. Minniti, C.A. Nelson, B.A. Peterson, P. Popowski, M.R. Pratt, P.J. Quinn, C.W. Stubbs, W. Sutherland, A.B. Tomaney, T. Vandehei, D.L. Welch, The MACHO Project 9 Million Star Color-Magnitude Diagram of the Large Magellanic Cloud. *Astron. J.* **119**, 2194–2213 (2000). doi: 10.1086/301326
- M. Barnabè, L.V.E. Koopmans, A Unifying Framework for Self-consistent Gravitational Lensing and Stellar Dynamics Analyses of Early-Type Galaxies. *Astrophys. J.* **666**, 726–746 (2007). doi: 10.1086/520495
- M. Barnabè, O. Czoske, L.V.E. Koopmans, T. Treu, A.S. Bolton, Two-dimensional kinematics of SLACS lenses - III. Mass structure and dynamics of early-type lens galaxies beyond $z \sim 0.1$. *Mon. Not. R. Astron. Soc.* **415**, 2215–2232 (2011). doi: 10.1111/j.1365-2966.2011.18842.x
- L.R. Bedin, G. Piotto, J. Anderson, S. Cassisi, I.R. King, Y. Momany, G. Carraro, ω Centauri: The Population Puzzle Goes Deeper. *Astrophys. J. Lett.* **605**, L125–L128 (2004). doi: 10.1086/420847
- M. Bellazzini, F.R. Ferraro, E. Pancino, Multiple stellar populations in the Sextans dwarf spheroidal galaxy? *Mon. Not. R. Astron. Soc.* **327**, L15–L20 (2001). doi: 10.1046/j.1365-8711.2001.04889.x
- M. Bellazzini, R.A. Ibata, S.C. Chapman, A.D. Mackey, L. Monaco, M.J. Irwin, N.F. Martin, G.F. Lewis, E. Dalessandro, The Nucleus of the Sagittarius Dsph Galaxy and M54: a Window on the Process of Galaxy Nucleation. *Astron. J.* **136**, 1147–1170, doi: 10.1088/0004-6256/136/3/1147 (2008)
- M. Bellazzini, G. Beccari, T.A. Oosterloo, S. Galleti, A. Sollima, M. Correnti, V. Testa, L. Mayer, M. Cignoni, F. Fraternali, S. Gallozzi, An optical and HI study of the dwarf Local Group galaxy VV124 = UGC4879. A gas-poor dwarf with a stellar disk? *Astron. Astrophys.* **527**, A58 (2011). doi: 10.1051/0004-6361/201016159
- E.J. Bernard, C. Gallart, M. Monelli, A. Aparicio, S. Cassisi, E.D. Skillman, P.B. Stetson, A.A. Cole, I. Drozdovsky, S.L. Hidalgo, M. Mateo, E. Tolstoy, The ACS LCID Project: RR Lyrae Stars as Tracers of Old Population Gradients in the Isolated Dwarf Spheroidal Galaxy Tucana. *Astrophys. J. Lett.* **678**, L21–L24 (2008). doi: 10.1086/588285
- E.J. Bernard, M. Monelli, C. Gallart, I. Drozdovsky, P.B. Stetson, A. Aparicio, S. Cassisi, L. Mayer, A.A. Cole, S.L. Hidalgo, E.D. Skillman, E. Tolstoy, The ACS LCID Project. I. Short-Period Variables in the Isolated Dwarf Spheroidal Galaxies Cetus and Tucana. *Astrophys. J.* **699**, 1742–1764 (2009). doi: 10.1088/0004-637X/699/2/1742
- E.J. Bernard, M. Monelli, C. Gallart, A. Aparicio, S. Cassisi, I. Drozdovsky, S.L. Hidalgo, E.D. Skillman, P.B. Stetson, The ACS LCID Project. II. Faint

- Variable Stars in the Isolated Dwarf Irregular Galaxy IC 1613. *Astrophys. J.* **712**, 1259–1276 (2010). doi: 10.1088/0004-637X/712/2/1259
- E.J. Bernard, M. Monelli, C. Gallart, G. Fiorentino, S. Cassisi, A. Aparicio, A.A. Cole, I. Drozdovsky, S.L. Hidalgo, E.D. Skillman, P.B. Stetson, E. Tolstoy, The ACS LCID Project – VIII. The short-period Cepheids of Leo A. *Mon. Not. R. Astron. Soc.* **432**, 3047–3061 (2013). doi: 10.1093/mnras/stt655
- S. Birrer, A. Amara, A. Refregier, Gravitational Lens Modeling with Basis Sets. *Astrophys. J.* **813**, 102 (2015). doi: 10.1088/0004-637X/813/2/102
- S. Birrer, A. Amara, A. Refregier, The mass-sheet degeneracy and time-delay cosmography: analysis of the strong lens RXJ1131-1231. *J. Cosmol. Astropart. Phys.* **8**, 020 (2016). doi: 10.1088/1475-7516/2016/08/020
- J.S. Bolton, M.G. Haehnelt, M. Viel, R.F. Carswell, Spatial fluctuations in the spectral shape of the ultraviolet background at $2 < z < 3$ and the reionization of helium. *Mon. Not. R. Astron. Soc.* **366**, 1378–1390 (2006). doi: 10.1111/j.1365-2966.2006.09927.x
- M. Bonamente, M.K. Joy, S.J. LaRoque, J.E. Carlstrom, E.D. Reese, K.S. Dawson, Determination of the Cosmic Distance Scale from Sunyaev–Zel’dovich Effect and Chandra X-Ray Measurements of High-Redshift Galaxy Clusters. *Astrophys. J.* **647**, 25–54 (2006). doi: 10.1086/505291
- G. Bono, F. Caputo, V. Castellani, M. Marconi, J. Storm, Theoretical insights into the RR Lyrae K-band period-luminosity relation. *Mon. Not. R. Astron. Soc.* **326**, 1183–1190 (2001). doi: 10.1046/j.1365-8711.2001.04655.x
- G. Bono, F. Caputo, V. Castellani, M. Marconi, J. Storm, S. Degl’Innocenti, A pulsational approach to near-infrared and visual magnitudes of RR Lyr stars. *Mon. Not. R. Astron. Soc.* **344**, 1097–1106 (2003). doi: 10.1046/j.1365-8711.2003.06878.x
- G. Bono, F. Caputo, M. Di Criscienzo, RR Lyrae stars in Galactic globular clusters. VI. The period-amplitude relation. *Astron. Astrophys.* **476**, 779–790 (2007) doi: 10.1051/0004-6361:20078206
- V. Bonvin, F. Courbin, S.H. Suyu, P.J. Marshall, C.E. Rusu, D. Sluse, M. Tewes, K.C. Wong, T. Collett, C.D. Fassnacht, T. Treu, M.W. Auger, S. Hilbert, L.V.E. Koopmans, G. Meylan, N. Rumbaugh, A. Sonnenfeld, C. Spiniello, H0LiCOW V. New COSMOGRAIL time delays of HE0435–1223: H_0 to 3.8% precision from strong lensing in a flat Λ CDM model. *Mon. Not. R. Astron. Soc.* **465**, 4914–4930 (2017). doi: 10.1093/mnras/stw3006
- C. Bot, N. Ysard, D. Paradis, J.P. Bernard, G. Lagache, F.P. Israel, W.F. Wall, Submillimeter to centimeter excess emission from the Magellanic Clouds. II. On the nature of the excess. *Astron. Astrophys.* **523**, A20 (2010). doi: 10.1051/0004-6361/201014986
- J.A. Braatz, M.J. Reid, E.M.L. Humphreys, C. Henkel, J.J. Condon, K.Y. Lo, The Megamaser Cosmology Project. II. The Angular-diameter Distance to UGC 3789. *Astrophys. J.* **718**, 657–665 (2010). doi: 10.1088/0004-637X/718/2/657
- R.S. Bussmann, D. Riechers, A. Fialkov, J. Scudder, C.C. Hayward, W.I. Cowley, J. Bock, J. Calanog, S.C. Chapman, A. Cooray, F. De Bernardis,

- D. Farrah, H. Fu, R. Gavazzi, R. Hopwood, R.J. Ivison, M. Jarvis, C. Lacey, A. Loeb, S.J. Oliver, I. Pérez-Fournon, D. Rigopoulou, I.G. Roseboom, D. Scott, A.J. Smith, L. Vieira, J.D. Wang, J. Wardlow, HerMES: ALMA Imaging of Herschel-selected Dusty Star-forming Galaxies. *Astrophys. J.* **812**, 43 (2015) doi: 10.1088/0004-637X/812/1/43
- C. Cacciari, G. Clementini, Globular Cluster Distances from RR Lyrae Stars. In: D. Alloin and W. Gieren (eds), *Stellar Candles for the Extragalactic Distance Scale*, Lect. Notes Phys., Springer, **635**, 105–122 (2003). doi: 10.1007/978-3-540-39882-0_6
- J.A.R. Caldwell, I.M. Coulson, The geometry and distance of the Magellanic Clouds from Cepheid variables. *Mon. Not. R. Astron. Soc.* **218**, 223–246 (1986). doi: 10.1093/mnras/218.2.223
- F. Caputo, V. Castellani, M. Marconi, V. Ripepi, Pulsational M_V versus $[\text{Fe}/\text{H}]$ relation(s) for globular cluster RR Lyrae variables. *Mon. Not. R. Astron. Soc.* **316**, 819–826 (2000). doi: 10.1046/j.1365-8711.2000.03591.x
- E. Carretta, R.G. Gratton, G. Clementini, F. Fusi Pecci, Distances, Ages, and Epoch of Formation of Globular Clusters. *Astrophys. J.* **533**, 215–235 (2000). doi: 10.1086/308629
- E. Carretta, A. Bragaglia, R. Gratton, V. D’Orazi, S. Lucatello, Intrinsic iron spread and a new metallicity scale for globular clusters. *Astron. Astrophys.* **508**, 695–706 (2009). doi: 10.1051/0004-6361/200913003
- S. Cassisi, M. Salaris, *Old Stellar Populations: How to Study the Fossil Record of Galaxy Formation*, Wiley-VCH (2013).
- M. Catelan, B.J. Pritzl, H.A. Smith, The RR Lyrae Period–Luminosity Relation. I. Theoretical Calibration. *Astrophys. J. Suppl. Ser.* **154**, 633–649 (2004). doi: 10.1086/422916
- M. Catelan, H.A. Smith, *Pulsating Stars* (Wiley-VCH) (2015).
- B. Chaboyer, Globular Cluster Distance Determinations. Post-Hipparcos Cosmic Candles. *Astrophys. Space Sci. Libr.* **237**, 111–124 (1999), doi: 10.1007/978-94-011-4734-7_7
- J.H.H. Chan, S.H. Suyu, T. Chiueh, A. More, P.J. Marshall, J. Coupon, M. Oguri, P. Price, Chitah: Strong-gravitational-lens Hunter in Imaging Surveys. *Astrophys. J.* **807** 138 (2015). doi: 10.1088/0004-637X/807/2/138
- G.C.F. Chen, S.H. Suyu, K.C. Wong, C.D. Fassnacht, T. Chiueh, A. Halkola, I. Hu, M.W. Auger, L.V.E. Koopmans, D.J. Lagattuta, J.P. McKean, S. Vegetti, SHARP – III: First Use Of Adaptive Optics Imaging To Constrain Cosmology With Gravitational Lens Time Delays. *Mon. Not. R. Astron. Soc.* **462**, 3457–3475 (2016). doi: 10.1093/mnras/stw991
- M. Cignoni, A.A. Cole, M. Tosi, J.S. Gallagher, E. Sabbi, J. Anderson, E.K. Grebel, A. Nota, Mean Age Gradient and Asymmetry in the Star Formation History of the Small Magellanic Cloud. *Astrophys. J.* **775**, 83 (2013). doi: 10.1088/0004-637X/775/2/83
- M.-R.L. Cioni, G. Clementini, L. Girardi, R. Guandalini, M. Gullieuszik, B. Miszalski, M.-I. Moretti, V. Ripepi, S. Rubele, G. Bagheri, K. Bekki, N. Cross, W.J.G. de Blok, R. de Grijs, J.P. Emerson, C.J. Evans, B. Gibson, E. Gonzales-Solares, M.A.T. Groenewegen, M. Irwin, V.D. Ivanov, J. Lewis,

- M. Marconi, J.-B. Marquette, C. Mastropietro, B. Moore, R. Napiwotzki, T. Naylor, J.M. Oliveira, M. Read, E. Sutorius, J.T. van Loon, M.I. Wilkinson, P.R. Wood, *Astron. Astrophys.* **527**, A116 (2011). doi: 10.1051/0004-6361/201016137
- G. Clementini, L. Federici, C. Corsi, C. Cacciari, M. Bellazzini, H.A. Smith, RR Lyrae Variables in the Globular Clusters of M31: A First Detection of Likely Candidates. *Astrophys. J. Lett.* **559**, L109–L112 (2001). doi: 10.1086/323973
- G. Clementini, R. Gratton, A. Bragaglia, E. Carretta, L. Di Fabrizio, M. Maio, Distance to the Large Magellanic Cloud: The RR Lyrae Stars. *Astron. J.* **125**, 1309–1329 (2003). doi: 10.1086/367773
- G. Clementini, M. Cignoni, R. Contreras Ramos, L. Federici, V. Ripepi, M. Marconi, M. Tosi, I. Musella, Variability and Star Formation in Leo T, the Lowest Luminosity Star-forming Galaxy Known Today. *Astrophys. J.* **756**, 108 (2012). doi: 10.1088/0004-637X/756/2/108
- A.A. Cole, E.D. Skillman, E. Tolstoy, J.S. Gallagher III, A. Aparicio, A.E. Dolphin, C. Gallart, S.L. Hidalgo, A. Saha, P.B. Stetson, D.R. Weisz, Leo A: A Late-blooming Survivor of the Epoch of Reionization in the Local Group. *Astrophys. J. Lett.* **659**, L17–L20 (2007). doi: 10.1086/516711
- A.A. Cole, D.R. Weisz, A.E. Dolphin, E.D. Skillman, A.W. McConnachie, A.M. Brooks, R. Leaman, Delayed Star Formation in Isolated Dwarf galaxies: Hubble Space Telescope Star Formation History of the Aquarius Dwarf Irregular. *Astrophys. J.* **795**, 54 (2014). doi: 10.1088/0004-637X/795/1/54
- T.E. Collett, M.W. Auger, Cosmological constraints from the double source plane lens SDSSJ0946+1006. *Mon. Not. R. Astron. Soc.* **443**, 969–976 (2014). doi: 10.1093/mnras/stu1190
- T.E. Collett, P.J. Marshall, M.W. Auger, S. Hilbert, S.H. Suyu, Z. Greene, T. Treu, C.D. Fassnacht, L.V.E. Koopmans, M. Bradač, R.D. Blandford, Reconstructing the lensing mass in the Universe from photometric catalogue data. *Mon. Not. R. Astron. Soc.* **432**, 679–692 (2013). doi: 10.1093/mnras/stt504
- M.L.M. Collins, S.C. Chapman, R.M. Rich, R.A. Ibata, N.F. Martin, M.J. Irwin, N.F. Bate, Lewis GF, Peñarrubia J, Arimoto N, Casey CM, Ferguson AMN, Koch A, A.W. McConnachie, N. Tanvir, A Kinematic Study of the Andromeda Dwarf Spheroidal System. *Astrophys. J.* **768**, 172 (2013). doi: 10.1088/0004-637X/768/2/172
- M.L.M. Collins, N.F. Martin, R.M. Rich, R.A. Ibata, S.C. Chapman, A.W. McConnachie, A.M. Ferguson, M.J. Irwin, G.F. Lewis, Comparing the Observable Properties of Dwarf Galaxies on and off the Andromeda Plane. *Astrophys. J. Lett.* **799**, L13 (2015). doi: 10.1088/2041-8205/799/1/L13
- A.R. Conn, R.A. Ibata, G.F. Lewis, Q.A. Parker, D.B. Zucker, N.F. Martin, A.W. McConnachie, M.J. Irwin, N. Tanvir, M.A. Fardal, A.M.N. Ferguson, S.C. Chapman, D. Valls-Gabaud, A Bayesian Approach to Locating the Red Giant Branch Tip Magnitude. II. Distances to the Satellites of M31. *Astrophys. J.* **758**, 11 (2012). doi: 10.1088/0004-637X/758/1/11

- G. Coppola, M. Marconi, P.B. Stetson, G. Bono, V.F. Braga, V. Ripepi, M. Dall’Ora, I. Musella, R. Buonanno, M. Fabrizio, I. Ferraro, G. Fiorentino, G. Iannicola, M. Monelli, M. Nonino, F. Thévenin, A.R. Walker, The Carina Project IX: On Hydrogen and Helium Burning Variables. *Astrophys. J.* **814**, 71 (2015). doi: 10.1088/0004-637X/814/1/71
- F. Courbin, P. Magain, M. Kirkove, S. Sohy, A Method for Spatial Deconvolution of Spectra. *Astrophys. J.* **529** 1136–1144 (2000). doi: 10.1086/308291
- F. Courbin, A. Eigenbrod, C. Vuissoz, G. Meylan, P. Magain, COSMOGRAIL: the COSmological MONitoring of GRAvItational Lenses. In: Y. Mellier and G. Meylan (eds), *Gravitational Lensing Impact on Cosmology*, Int’l Astron. Union Symp. **225**, 297–303 (2005). doi: 10.1017/S1743921305002097
- F. Courbin, V. Chantry, Y. Revaz, D. Sluse, C. Faure, M. Tewes, E. Eulaers, M. Koleva, I. Asfandiyarov, S. Dye, P. Magain, H. van Winckel, J. Coles, P. Saha, M. Ibrahimov, G. Meylan, COSMOGRAIL: the COSmological MONitoring of GRAvItational Lenses. IX. Time delays, lens dynamics and baryonic fraction in HE 0435-1223. *Astron. Astrophys.* **536**, A53 (2011). doi: 10.1051/0004-6361/201015709
- S. Crandall, B. Ratra, Non-Gaussian Error Distributions of LMC Distance Moduli Measurements. *Astrophys. J.* **815**, 87 (2015). doi: 10.1088/0004-637X/815/2/87
- H.H. Crowl, A. Sarajedini, A.E. Piatti, D. Geisler, E. Bica, J.J. Clariá, J.F.C. Santos Jr., The Line-of-Sight Depth of Populous Clusters in the Small Magellanic Cloud. *Astron. J.* **122**, 220–231 (2001). doi: 10.1086/321128
- F. Cusano, G. Clementini, A. Garofalo, M. Cignoni, L. Federici, M. Marconi, I. Musella, V. Ripepi, K. Boutsia, M. Fumana, S. Gallozzi, V. Testa, Dwarf Spheroidal Satellites of M31. I. Variable Stars and Stellar Populations in Andromeda XIX. *Astrophys. J.* **779**, 7 (2013). doi: 10.1088/0004-637X/779/1/7
- F. Cusano, A. Garofalo, G. Clementini, M. Cignoni, L. Federici, M. Marconi, I. Musella, V. Ripepi, R. Speziali, E. Sani, R. Merighi, Variable Stars and Stellar Populations in Andromeda XXI. II. Another Merged Galaxy Satellite of M31? *Astrophys. J.* **806**, 200 (2015). doi: 10.1088/0004-637X/806/2/200
- G.S. Da Costa, T.E. Armandroff, Standard globular cluster giant branches in the $(M_I, V - I_0)$ plane. *Astron. J.* **100**, 162–181 (1990). doi: 10.1086/115500
- G.S. Da Costa, T.E. Armandroff, N. Caldwell, P. Seitzer, The Dwarf Spheroidal Companions to M31: WFPC2 Observations of Andromeda I. *Astron. J.* **112**, 2576–2595 (1996). doi: 10.1086/118204
- G.S. Da Costa, T.E. Armandroff, N. Caldwell, P. Seitzer, The Dwarf Spheroidal Companions to M31: WFPC2 Observations of Andromeda II. *Astron. J.* **119**, 705–726 (2000). doi: 10.1086/301223
- G.S. Da Costa, T.E. Armandroff, N. Caldwell, The Dwarf Spheroidal Companions to M31: WFPC2 Observations of Andromeda III. *Astron. J.* **124**, 332–348 (2002). doi: 10.1086/340965
- G.S. Da Costa, M. Rejkuba, H. Jerjen, E.K. Grebel, Ancient Stars Beyond the Local Group: RR Lyrae Variables and Blue Horizontal Branch Stars in Sculptor Group Dwarf Galaxies. *Astrophys. J. Lett.* **708**, L121–L125 (2010). doi: 10.1088/2041-8205/708/2/L121

- N. Dalal, D.E. Holz, S.A. Hughes, B. Jain, Short GRB and binary black hole standard sirens as a probe of dark energy. *Phys. Rev. D* **74**, 063006 (2006). doi: 10.1103/PhysRevD.74.063006
- Dark Energy Survey Collaboration: T. Abbott, F.B. Abdalla, J. Aleksić, S. Allam, A. Amara, D. Bacon, E. Balbinot, M. Banerji, K. Bechtol, A. Benoit-Lévy, G.M. Bernstein, E. Bertin, J. Blazek, C. Bonnett, S. Bridle, D. Brooks, R.J. Brunner, E. Buckley-Geer, D.L. Burke, G.B. Caminha, D. Capozzi, J. Carlsen, A. Carnero-Rosell, M. Carollo, M. Carrasco-Kind, J. Carretero, F.J. Castander, L. Clerkin, T. Collett, C. Conselice, M. Crocce, C.E. Cunha, C.B. D’Andrea, L.N. da Costa, T.M. Davis, S. Desai, H.T. Diehl, J.P. Dietrich, S. Dodelson, P. Doel, A. Drlica-Wagner, J. Estrada, J. Etherington, A.E. Evrard, J. Fabbri, D.A. Finley, B. Flaugher, R.J. Foley, P. Fosalba, J. Frieman, J. García-Bellido, E. Gaztanaga, D.W. Gerdes, T. Giannantonio, D.A. Goldstein, D. Gruen, R.A. Gruendl, P. Guarnieri, G. Gutierrez, W. Hartley, K. Honscheid, B. Jain, D.J. James, T. Jeltema, S. Jovel, R. Kessler, A. King, D. Kirk, R. Kron, K. Kuehn, N. Kuropatkin, O. Lahav, T.S. Li, M. Lima, H. Lin, M.A.G. Maia, M. Makler, M. Manera, C. Maraston, J.L. Marshall, P. Martini, R.G. McMahon, P. Melchior, A. Merson, C.J. Miller, R. Miquel, J.J. Mohr, X. Morice-Atkinson, K. Naidoo, E. Neilsen, R.C. Nichol, B. Nord, R. Ogando, F. Ostrovski, A. Palmese, A. Papadopoulos, H.V. Peiris, J. Peoples, W.J. Percival, A.A. Plazas, S.L. Reed, A. Refregier, A.K. Romer, A. Roodman, A. Ross, E. Roza, E.S. Rykoff, I. Sadeh, M. Sako, C. Sánchez, E. Sanchez, B. Santiago, V. Scarpine, M. Schubnell, I. Sevilla-Noarbe, E. Sheldon, M. Smith, R.C. Smith, M. Soares-Santos, F. Sobreira, M. Soumagnac, E. Suchyta, M. Sullivan, M. Swanson, G. Tarle, J. Thaler, D. Thomas, R.C. Thomas, D. Tucker, J.D. Vieira, V. Vikram, A.R. Walker, R.H. Wechsler, J. Weller, W. Wester, L. Whiteway, H. Wilcox, B. Yanny, Y. Zhang, J. Zuntz, The Dark Energy Survey: more than dark energy – an overview. *Mon. Not. R. Astron. Soc.* **460**, 1270–1299 (2016). doi: 10.1093/mnras/stw641
- T.J.L. de Boer, E. Tolstoy, V. Hill, A. Saha, K. Olsen, E. Starkenburg, B. Lemasle, M.J. Irwin, G. Battaglia, The star formation and chemical evolution history of the sculptor dwarf spheroidal galaxy. *Astron. Astrophys.* **539**, A103 (2012). doi: 10.1051/0004-6361/201118378
- R. de Grijs, *An Introduction to Distance Measurement in Astronomy*, Wiley-Blackwell Acad. Publ. (2011).
- R. de Grijs, Advancing the physics of cosmic distances: Conference summary. In: *Advancing the Physics of Cosmic Distances*, Int’l Astron. Union Symp. **289** 351–360 (2013). doi: 10.1017/S1743921312021709
- R. de Grijs, J.E. Wicker, G. Bono, Clustering of Local Group Distances: Publication Bias or Correlated Measurements? I. The Large Magellanic Cloud. *Astron. J.* **147**, 122 (2014). doi: 10.1088/0004-6256/147/5/122
- R. de Grijs, G. Bono, Clustering of Local Group Distances: Publication Bias or Correlated Measurements? II. M31 and Beyond. *Astron. J.* **148**, 117 (2014). doi: 10.1088/0004-6256/148/1/17

- R. de Grijs, G. Bono, Clustering of Local Group Distances: Publication Bias or Correlated Measurements? III. The Small Magellanic Cloud. *Astron. J.* **149**, 179 (2015). doi: 10.1088/0004-6256/149/6/179
- R. de Grijs, G. Bono, Clustering of Local Group Distances: Publication Bias or Correlated Measurements? IV. The Galactic Center. *Astrophys. J. Suppl. Ser.* **227**, 5 (2016). doi: 10.3847/0067-0049/227/1/5
- K. Dobashi, J.-P. Bernard, A. Kawamura, F. Egusa, A. Hughes, D. Paradis, C. Bot, W.T. Reach, Extinction Map of the Small Magellanic Cloud Based on the SIRIUS and 6X 2MASS Point Source Catalogs. *Astron. J.* **137**, 5099–5109 (2009). doi: 10.1088/0004-6256/137/6/5099
- E. D’Onghia, G. Besla, T.J. Cox, L. Hernquist, Resonant stripping as the origin of dwarf spheroidal galaxies. *Nature* **460**, 605–607 (2009). doi: 10.1038/nature08215
- S. Dye, S.J. Warren, Decomposition of the Visible and Dark Matter in the Einstein Ring 0047–2808 by Semilinear Inversion. *Astrophys. J.* **623**, 31–41 (2005). doi: 10.1086/428340
- A. Eigenbrod, F. Courbin, C. Vuissoz, G. Meylan, P. Saha, S. Dye, COSMOGRAIL: The COSmological MONitoring of GRAvItational Lenses. I. How to sample the light curves of gravitationally lensed quasars to measure accurate time delays. *Astron. Astrophys.* **436**, 25–35 (2005). doi: 10.1051/0004-6361:20042422
- A. Eigenbrod, F. Courbin, G. Meylan, C. Vuissoz, P. Magain, COSMOGRAIL: the COSmological MONitoring of GRAvItational Lenses. III. Redshift of the lensing galaxy in eight gravitationally lensed quasars. *Astron. Astrophys.* **451**, 759–766 (2006). doi: 10.1051/0004-6361:20054454
- A. Eigenbrod, F. Courbin, G. Meylan, COSMOGRAIL: the COSmological MONitoring of GRAvItational Lenses. VI. Redshift of the lensing galaxy in seven gravitationally lensed quasars. *Astron. Astrophys.* **465**, 51–56 (2007). doi: 10.1051/0004-6361:20066939
- J.D. Ellithorpe, C.S. Kochanek, J.N. Hewitt, Visibility LensClean and the Reliability of Deconvolved Radio Images. *Astrophys. J.* **464**, 556–567 (1996). doi: 10.1086/177346
- R. Fadely, C.R. Keeton, R. Nakajima, G.M. Bernstein, Improved Constraints on the Gravitational Lens Q0957+561. II. Strong Lensing. *Astrophys. J.* **711**, 246–267 (2010). doi: 10.1088/0004-637X/711/1/246
- E.E. Falco, M.V. Gorenstein, I.I. Shapiro, On model-dependent bounds on H_0 from gravitational images Application of Q0957+561A,B. *Astrophys. J. Lett.* **289**, L1–L4 (1985). doi: 10.1086/184422
- C.D. Fassnacht, L.V.E. Koopmans, K.C. Wong, Galaxy number counts and implications for strong lensing. *Mon. Not. R. Astron. Soc.* **410**, 2167–2179 (2011). doi: 10.1111/j.1365-2966.2010.17591.x
- A.M.N. Ferguson, A.D. Mackey, Substructure and Tidal Streams in the Andromeda Galaxy and its Satellites. In: H.J. Newberg and J.L. Carlin (eds), *Astrophys. Space Sci. Libr.* **420**, 191–217 (2016). doi: 10.1007/978-3-319-19336-6_8

- L. Ferrarese, J.R. Mould, R.C. Kennicutt Jr., J. Huchra, H.C. Ford, W.L. Freedman, P.B. Stetson, B.F. Madore, S. Sakai, B.K. Gibson, J.A. Graham, S.M. Hughes, G.D. Illingworth, D.D. Kelson, L. Macri, K. Sebo, N.A. Silbermann, The Hubble Space Telescope Key Project on the Extragalactic Distance Scale. XXVI. The Calibration of Population II Secondary Distance Indicators and the Value of the Hubble Constant. *Astrophys. J.* **529**, 745–767 (2000). doi: 10.1086/308309
- G. Fiorentino, M. Limongi, F. Caputo, M. Marconi, Synthetic properties of bright metal-poor variables. I. ‘Anomalous’ Cepheids. *Astron. Astrophys.* **460**, 155–166 (2006). doi: 10.1051/0004-6361:20065349
- G. Fiorentino, A. Monachesi, S.C. Trager, T.R. Lauer, A. Saha, K.J. Mighell, W. Freedman, A. Dressler, C. Grillmair, E. Tolstoy, RR Lyrae Variables in M32 and the Disk of M31. *Astrophys. J.* **708**, 817–833 (2010). doi: 10.1088/0004-637X/708/1/817
- G. Fiorentino, R. Contreras Ramos, E. Tolstoy, G. Clementini, A. Saha, The ancient stellar population of M32: RR Lyrae variable stars confirmed. *Astron. Astrophys.* **539**, A138 (2012a). doi: 10.1051/0004-6361/201117434
- G. Fiorentino, P.B. Stetson, M. Monelli, G. Bono, E.J. Bernard, A. Pietrinferni, On the Central Helium-burning Variable Stars of the LeoI Dwarf Spheroidal Galaxy. *Astrophys. J. Lett.* **759** L12 (2012b). doi: 10.1088/2041-8205/759/1/L12
- G. Fiorentino, G. Bono, M. Monelli, P.B. Stetson, E. Tolstoy, C. Gallart, M. Salaris, C.E. Martínez-Vásquez, E.J. Bernard, Weak Galactic Halo-Dwarf Spheroidal Connection from RR Lyrae Stars. *Astrophys. J. Lett.* **798**, L12 (2015). doi: 10.1088/2041-8205/798/1/L12
- B. Flaugher, H.T. Diehl, K. Honscheid, T.M.C. Abbott, O. Alvarez, R. Angstadt, J.T. Annis, M. Antonik, O. Ballester, L. Beaufore, G.M. Bernstein, R.A. Bernstein, B. Bigelow, M. Bonati, D. Boprie, D. Brooks, E.J. Buckley-Geer, J. Campa, L. Cardiel-Sas, F.J. Castander, J. Castilla, H. Cease, J.M. Cela-Ruiz, S. Chappa, E. Chi, C. Cooper, L.N. da Costa, E. Dede, G. Derylo, D.L. DePoy, J. de Vicente, P. Doel, A. Drlica-Wagner, J. Eiting, A.E. Elliott, J. Emes, J. Estrada, A. Fausti Neto, D.A. Finley, R. Flores, J. Frieman, D. Gerdes, M.D. Gladders, B. Gregory, G.R. Gutierrez, J. Hao, S.E. Holland, S. Holm, D. Huffman, C. Jackson, D.J. James, M. Jonas, A. Karcher, I. Karliner, S. Kent, R. Kessler, M. Kozlovsky, R.G. Kron, D. Kubik, K. Kuehn, S. Kuhlmann, K. Kuk, O. Lahav, A. Lathrop, J. Lee, M.E. Levi, P. Lewis, T.S. Li, I. Mandrichenko, J.L. Marshall, G. Martinez, K.W. Merritt, R. Miquel, F. Muñoz, E.H. Neilsen, R.C. Nichol, B. Nord, R. Ogando, J. Olsen, N. Palaio, K. Patton, J. Peoples, A.A. Plazas, J. Rauch, K. Reil, J.P. Rheault, N.A. Roe, H. Rogers, A. Roodman, E. Sanchez, V. Scarpine, R.H. Schindler, R. Schmidt, R. Schmitt, M. Schubnell, K. Schultz, P. Schurter, L. Scott, S. Serrano, T.M. Shaw, R.C. Smith, M. Soares-Santos, A. Stefanik, W. Stuermer, E. Suchyta, A. Sypniewski, G. Tarle, J. Thaler, R. Tighe, C. Tran, D. Tucker, A.R. Walker, G. Wang, M. Watson, C. Weaverdyck, W. Wester, R. Woods, B. Yanny, DES Collaboration, The Dark Energy Camera. *Astron. J.* **150**, 150 (2015). doi:

- 10.1088/0004-6256/150/5/150
- T. Foster, B. Cooper, Structure and Dynamics of the Milky Way: The Evolving Picture. In: *The Dynamic Interstellar Medium: A Celebration of the Canadian Galactic Plane Survey*, R. Kothes, T.L. Landecker, A.G. Willis (eds), *Astron. Soc. Pac. Conf. Proc.* **438**, 16–30 (2010).
- C. Francis, E. Anderson, Two estimates of the distance to the Galactic Centre. *Mon. Not. R. Astron. Soc.* **441**, 1105–1114 (2014). doi: 10.1093/mnras/stu631
- F. Fraternali, E. Tolstoy, M.J. Irwin, A.A. Cole, Life at the periphery of the Local Group: the kinematics of the Tucana dwarf galaxy. *Astron. Astrophys.* **499**, 121–128 (2009). doi: 10.1051/0004-6361/200810830
- W.L. Freedman, B.F. Madore, B.K. Gibson, L. Ferrarese, D.D. Kelson, S. Sakai, J.R. Mould, R.C. Kennicutt Jr., H.C. Ford, J.A. Graham, J.P. Huchra, S.M.G. Hughes, G.D. Illingworth, L.M. Macri, P.B. Stetson, Final Results from the Hubble Space Telescope Key Project to Measure the Hubble Constant. *Astrophys. J.* **553**, 47–72 (2001). doi: 10.1086/320638
- W.L. Freedman, B.F. Madore, V. Scowcroft, C. Burns, A. Monson, S.E. Persson, M. Seibert, J. Rigby, Carnegie Hubble Program: A Mid-infrared Calibration of the Hubble Constant. *Astrophys. J.* **758**, 24 (2012). doi: 10.1088/0004-637X/758/1/24
- C. Gallart, A. Aparicio, W.L. Freedman, B.F. Madore, D. Martínez-Delgado, P.B. Stetson, The Variable-Star Population in Phoenix: Coexistence of Anomalous and Short-Period Classical Cepheids and Detection of RR Lyrae Variables. *Astron. J.* **127**, 1486–1501 (2004). doi: 10.1086/381955
- C. Gallart, M. Monelli, L. Mayer, A. Aparicio, G. Battaglia, E.J. Bernard, S. Cassisi, A.A. Cole, A.E. Dolphin, I. Drozdovsky, S.L. Hidalgo, J.F. Navarro, S. Salvadori, E.D. Skillman, P.B. Stetson, D.R. Weisz, The ACS LCID Project: On the Origin of Dwarf Galaxy Types – A Manifestation of the Halo Assembly Bias? *Astrophys. J. Lett.* **811**, L18 (2015). doi: 10.1088/2041-8205/811/2/L18
- R. Gavazzi, P.J. Marshall, T. Treu, A. Sonnenfeld, RINGFINDER: Automated Detection of Galaxy-scale Gravitational Lenses in Ground-based Multi-filter Imaging Data. *Astrophys. J.* **785**, 144 (2014). doi: 10.1088/0004-637X/785/2/144
- M.V. Gorenstein, I.I. Shapiro, E.E. Falco, Degeneracies in parameter estimates for models of gravitational lens systems. *Astrophys. J.* **327**, 693–711 (1988). doi: 10.1086/166226
- D. Graczyk, G. Pietrzyński, I.B. Thompson, W. Gieren, B. Pilecki, P. Konorski, A. Udalski, I. Soszyński, S. Villanova, M. Górski, K. Suchomska, P. Karczmarek, R.-P. Kudritzki, F. Bresolin, A. Gallenne, The Araucaria Project. The Distance to the Small Magellanic Cloud from Late-type Eclipsing Binaries. *Astrophys. J.* **780**, 59 (2014). doi: 10.1088/0004-637X/780/1/59
- R.G. Gratton, A. Bragaglia, G. Clementini, E. Carretta, L. Di Fabrizio, M. Maio, E. Taribello, Metal abundances of RR Lyrae stars in the bar of the Large Magellanic Cloud. *Astron. Astrophys.* **421**, 937–952 (2004). doi:

- 10.1051/0004-6361:20035840
- Z.S. Greene, S.H. Suyu, T. Treu, S. Hilbert, M.W. Auger, T.E. Collett, P.J. Marshall, C.D. Fassnacht, R.D. Blandford, M. Bradač, L.V.E. Koopmans, Improving the Precision of Time-delay Cosmography with Observations of Galaxies along the Line of Sight. *Astrophys. J.* **768**, 39 (2013) doi: 10.1088/0004-637X/768/1/39
- M.A.T. Groenewegen, LMC and SMC Cepheids: combining OGLE with DENIS and 2MASS infrared data. *Astron. Astrophys.* **363**, 901–916 (2000).
- R. Haschke, E.K. Grebel, S. Duffau, Three-dimensional Maps of the Magellanic Clouds using RR Lyrae Stars and Cepheids. II. The Small Magellanic Cloud. *Astron. J.* **144**, 107 (2012). doi: 10.1088/0004-6256/144/4/107
- D. Hatt, R.L. Beaton, W.L. Freedman, B.F. Madore, I.S. Jang, T.J. Hoyt, M.G. Lee, A.J. Monson, J.A. Rich, V. Scowcroft, M. Seibert, The Carnegie–Chicago Hubble Program. II. The Distance to IC 1613: The Tip of the Red Giant Branch and RR Lyrae Period–Luminosity Relations. *Astrophys. J.* submitted (arXiv:1703.06468) (2017).
- J.R. Herrnstein, J.M. Moran, L.J. Greenhill, P.J. Diamond, M. Inoue, N. Nakai, M. Miyoshi, C. Henkel, A. Riess, A geometric distance to the galaxy NGC4258 from orbital motions in a nuclear gas disk. *Nature* **400**, 539–541 (1999). 10.1038/22972
- Y.D. Hezaveh, D.P. Marrone, C.D. Fassnacht, J.S. Spilker, J.D. Vieira, J.E. Aguirre, K.A. Aird, M. Aravena, M.L.N. Ashby, M. Bayliss, B.A. Benson, L.E. Bleem, M. Bothwell, M. Brodwin, J.E. Carlstrom, C.L. Chang, S.C. Chapman, T.M. Crawford, A.T. Crites, C. De Breuck, T. de Haan, M.A. Dobbs, E.B. Fomalont, E.M. George, M.D. Gladders, A.H. Gonzalez, T.R. Greve, N.W. Halverson, F.W. High, G.P. Holder, W.L. Holzapfel, S. Hoover, J.D. Hrubes, K. Husband, T.R. Hunter, R. Keisler, A.T. Lee, E.M. Leitch, M. Lueker, D. Luong-Van, M. Malkan, V. McIntyre, J.J. McMahon, J. Mehl, K.M. Menten, S.S. Meyer, L.M. Mocanu, E.J. Murphy, T. Natoli, S. Padin, T. Plagge, C.L. Reichardt, A. Rest, J. Ruel, J.E. Ruhl, K. Sharon, K.K. Schaffer, L. Shaw, E. Shirokoff, B. Stalder, Z. Staniszewski, A.A. Stark, K. Story, K. Vanderlinde, A. Weiß, N. Welikala, R. Williamson, ALMA Observations of SPT-discovered, Strongly Lensed, Dusty, Star-forming Galaxies. *Astrophys. J.* **767**, 132 (2013). doi: 10.1088/0004-637X/767/2/132
- Y.D. Hezaveh, N. Dalal, D.P. Marrone, Y.Y. Mao, W. Morningstar, D. Wen, R.D. Blandford, J.E. Carlstrom, C.D. Fassnacht, G.P. Holder, A. Kembball, P.J. Marshall, N. Murray, L. Perreault Levasseur, J.D. Vieira, R.H. Wechsler, Detection of Lensing Substructure Using ALMA Observations of the Dusty Galaxy SDP.81. *Astrophys. J.* **823**, 37 (2016). doi: 10.3847/0004-637X/823/1/37
- S.L. Hidalgo, A. Aparicio, D. Martínez-Delgado, C. Gallart, On the Extended Structure of the Phoenix Dwarf Galaxy. *Astrophys. J.* **705**, 704–716 (2009). doi: 10.1088/0004-637X/705/1/704
- S. Hilbert, S.D.M. White, J. Hartlap, P. Schneider, Strong lensing optical depths in a Λ CDM universe. *Mon. Not. R. Astron. Soc.* **382**, 121–132 (2007). doi: 10.1111/j.1365-2966.2007.12391.x

- S. Hilbert, J. Hartlap, S.D.M. White, P. Schneider, Ray-tracing through the Millennium Simulation: Born corrections and lens-lens coupling in cosmic shear and galaxy-galaxy lensing. *Astron. Astrophys.* **499**, 31–43 (2009). doi: 10.1051/0004-6361/200811054
- Hitomi Collaboration, F. Aharonian, et al., The quiescent intracluster medium in the core of the Perseus cluster. *Nature* **535**, 117–121 (2016). doi: 0.1038/nature18627
- N. Ho, M. Geha, R.R. Munoz, P. Guhathakurta, J. Kalirai, K.M. Gilbert, E. Tollerud, J. Bullock, R.L. Beaton, S.R. Majewski, Stellar Kinematics of the Andromeda II Dwarf Spheroidal Galaxy. *Astrophys. J.* **758**, 124 (2012). doi: 10.1088/0004-637X/758/2/124
- N. Ho, M. Geha, E.J. Tollerud, R. Zinn, P. Guhathakurta, L.C. Vargas, Metallicity Evolution of the Six Most Luminous M31 Dwarf Satellites. *Astrophys. J.* **798**, 77 (2015). doi: 10.1088/0004-637X/798/2/77
- D.E. Holz, S.A. Hughes, Using Gravitational-Wave Standard Sirens. *Astrophys. J.* **629**, 15–22 (2005). doi: 10.1086/431341
- R. Ibata, M. Irwin, G. Lewis, A.M.N. Ferguson, N. Tanvir, A giant stream of metal-rich stars in the halo of the galaxy M31. *Nature* **412**, 49–52 (2001).
- N. Inada, M. Oguri, M.S. Shin, I. Kayo, M.A. Strauss, T. Morokuma, C.E. Rusu, M. Fukugita, C.S. Kochanek, G.T. Richards, D.P. Schneider, D.G. York, N.A. Bahcall, J.A. Frieman, P.B. Hall, R.L. White, The Sloan Digital Sky Survey Quasar Lens Search. V. Final Catalog from the Seventh Data Release. *Astron. J.* **143**, 119 (2012). doi: 10.1088/0004-6256/143/5/119
- L. Inno, N. Matsunaga, G. Bono, F. Caputo, R. Buonanno, K. Genovali, C.D. Laney, M. Marconi, A.M. Piersimoni, F. Primas, M. Romaniello, On the Distance of the Magellanic Clouds Using Cepheid NIR and Optical–NIR Period–Wesenheit Relations. *Astrophys. J.* **764**, 84 (2013). doi: 10.1088/0004-637X/764/1/84
- L. Inno, G. Bono, N. Matsunaga, G. Fiorentino, M. Marconi, B. Lemasle, R. da Silva, I. Soszyński, A. Udalski, M. Romaniello, H.-W. Rix, The Panchromatic View of the Magellanic Clouds from Classical Cepheids. I. Distance, Reddening, and Geometry of the Large Magellanic Cloud Disk. *Astrophys. J.* **832**, 176 (2016). doi: 10.3847/0004-637X/832/2/176
- N. Jackson, H. Rampadarath, E.O. Ofek, M. Oguri, M.S. Shin, New lensed quasars from the MUSCLES survey. *Mon. Not. R. Astron. Soc.* **419**, 2014–2024 (2012). doi: 10.1111/j.1365-2966.2011.19857.x
- I. Jee, E. Komatsu, S.H. Suyu, Measuring angular diameter distances of strong gravitational lenses. *J. Cosmol. Astropart. Phys.* **2015**(11), 033 (2015). doi: 10.1088/1475-7516/2015/11/033
- I. Jee, E. Komatsu, S.H. Suyu, D. Huterer, Time-delay Cosmography: Increased Leverage with Angular Diameter Distances. *J. Cosmol. Astropart. Phys.* **2016**(04), 031 (2016). doi: 10.1088/1475-7516/2016/04/031
- E.J. Jeffery, E. Smith, T.M. Brown, A.V. Sweigart, J.S. Kalirai, H.C. Ferguson, P. Guhathakurta, A. Renzini, R.M. Rich, HST/ACS Observations of RR Lyrae Stars in Six Ultra-deep Fields of M31. *Astron. J.* **141**, 171 (2011). doi: 10.1088/0004-6256/141/5/171

- R. Jimenez, A. Loeb, Constraining Cosmological Parameters Based on Relative Galaxy Ages. *Astrophys. J.* **573**, 37–42 (2002). doi: 10.1086/340549
- R. Jimenez, L. Verde, T. Treu, D. Stern, Constraints on the Equation of State of Dark Energy and the Hubble Constant from Stellar Ages and the Cosmic Microwave Background. *Astrophys. J.* **593**, 622–629 (2003). doi: 10.1086/376595
- R. Joseph, F. Courbin, R.B. Metcalf, C. Giocoli, P. Hartley, N. Jackson, F. Bellagamba, J.P. Kneib, L. Koopmans, G. Lemson, M. Meneghetti, G. Meylan, M. Petkova, S. Pires, A PCA-based automated finder for galaxy-scale strong lenses. *Astron. Astrophys.* **566**, A63 (2014). doi: 10.1051/0004-6361/201423365
- E. Jullo, J.P. Kneib, Multiscale cluster lens mass mapping – I. Strong lensing modelling. *Mon. Not. R. Astron. Soc.* **395**, 1319–1332 (2009). doi: 10.1111/j.1365-2966.2009.14654.x
- E. Jullo, J. Kneib, M. Limousin, Á. Elíasdóttir, P.J. Marshall, T. Verdugo, A Bayesian approach to strong lensing modelling of galaxy clusters. *New J. Phys.* **9**, 447 (2007). doi: 10.1088/1367-2630/9/12/447
- J.S. Kalirai, R.L. Beaton, M.C. Geha, K.M. Gilbert, P. Guhathakurta, E.N. Kirby, S.R. Majewski, J.C. Ostheimer, R.J. Patterson, J. Wolf, The SPLASH Survey: Internal Kinematics, Chemical Abundances, and Masses of the Andromeda I, II, III, VII, X, and XIV Dwarf Spheroidal Galaxies. *Astrophys. J.* **711**, 671–692 (2010). doi: 10.1088/0004-637X/711/2/671
- J.S. Kalirai, J. Anderson, A. Dotter, H.B. Richer, G.G. Fahlman, B.M.S. Hansen, J. Hurley, I.N. Reid, R.M. Rich, M.M. Shara, Ultra-Deep Hubble Space Telescope Imaging of the Small Magellanic Cloud: The Initial Mass Function of Stars with $M \lesssim 1M_{\odot}$. *Astrophys. J.* **763**, 110 (2013). doi: 10.1088/0004-637X/763/2/110
- E. Kapakos, D. Hatzidimitriou, RR Lyrae variables in the Small Magellanic Cloud – II. The extended area: chemical and structural analysis. *Mon. Not. R. Astron. Soc.* **426**, 2063–2077 (2012). doi: 10.1111/j.1365-2966.2012.21834.x
- H. Kawahara, T. Kitayama, S. Sasaki, Y. Suto, Systematic Errors in the Hubble Constant Measurement from the Sunyaev-Zel’dovich Effect. *Astrophys. J.* **674**, 11–21 (2008). doi: 10.1086/524132
- I. Kayo, N. Inada, M. Oguri, T. Morokuma, P.B. Hall, C.S. Kochanek, D.P. Schneider, Eight New Quasar Lenses from the Sloan Digital Sky Survey Quasar Lens Search. *Astron. J.* **139**, 1614–1621 (2010). doi: 10.1088/0004-6256/139/4/1614
- K. Kinemuchi, H.C. Harris, H.A. Smith, N.A. Silbermann, L.A. Snyder, A.P. La Cluyzé, C.L. Clark, The Variable Stars of the Draco Dwarf Spheroidal Galaxy: Revisited. *Astron. J.* **136**, 1921–1939 (2008). doi: 10.1088/0004-6256/136/5/1921
- J.P. Kneib, J.G. Cohen, J. Hjorth, RX J0911+05: A Massive Cluster Lens at $z = 0.769$. *Astrophys. J. Lett.* **544**, L35–L39 (2000). doi: 10.1086/317285
- C.S. Kochanek, R. Narayan, LensClean: an algorithm for inverting extended, gravitationally lensed images with application to the radio ring lens PKS

- 1830–211. *Astrophys. J.* **401**, 461–473 (1992). doi: 10.1086/172078
- C.S. Kochanek, C.R. Keeton, B.A. McLeod, The Importance of Einstein Rings. *Astrophys. J.* **547**, 50–59 (2001). doi: 10.1086/318350
- C.S. Kochanek, B. Mochejska, N.D. Morgan, K.Z. Stanek, A Simple Method to Find All Lensed Quasars. *Astrophys. J. Lett.* **637**, L73–L76 (2006). doi: 10.1086/500559
- C.H.B. Koenig, J.M. Nemec, J.R. Mould, G.G. Fahlman, Color–magnitude diagram for the Andromeda II dwarf galaxy. *Astron. J.* **106**, 1819–1825 (1993). doi: 10.1086/116767
- L.V.E. Koopmans, T. Treu, C.D. Fassnacht, R.D. Blandford, G. Surpi, The Hubble Constant from the Gravitational Lens B1608+656. *Astrophys. J.* **599**, 70–85 (2003). doi: 10.1086/379226
- K. Kuijken, C. Heymans, H. Hildebrandt, R. Nakajima, T. Erben, J.T.A. de Jong, M. Viola, A. Choi, H. Hoekstra, L. Miller, E. van Uitert, A. Amon, C. Blake, M. Brouwer, A. Buddendiek, I.F. Conti, M. Eriksen, A. Grado, J. Harnois-Déraps, E. Helmich, R. Herbonnet, N. Irisarri, T. Kitching, D. Klaes, F. La Barbera, N. Napolitano, M. Radovich, P. Schneider, C. Sifón, G. Sikkema, P. Simon, A. Tudorica, E. Valentijn, G. Verdoes Kleijn, L. van Waerbeke, Gravitational lensing analysis of the Kilo-Degree Survey. *Mon. Not. R. Astron. Soc.* **454**, 3500–3532 (2015). doi: 10.1093/mnras/stv2140
- C.Y. Kuo, J.A. Braatz, M.J. Reid, K.Y. Lo, J.J. Condon, C.M.V. Impellizzeri, C. Henkel, The Megamaser Cosmology Project. V. An Angular-diameter Distance to NGC 6264 at 140 Mpc. *Astrophys. J.* **767**, 155 (2013). doi: 10.1088/0004-637X/767/2/155
- C.D. Laney, R.S. Stobie, Infrared photometry of Magellanic Cloud Cepheids - Intrinsic properties of Cepheids and the spatial structure of Clouds. *Mon. Not. R. Astron. Soc.* **222**, 449–472 (1986). doi: 10.1093/mnras/222.3.449
- R. Laureijs, J. Amiaux, S. Arduini, J. Auguères, J. Brinchmann, R. Cole, M. Cropper, C. Dabin, L. Duvet, A. Ealet, et al., Euclid Definition Study Report. *ArXiv:1110.3193* (2011).
- M.G. Lee, W.L. Freedman, B.F. Madore, The Tip of the Red Giant Branch as a Distance Indicator for Resolved Galaxies. *Astrophys. J.* **417**, 553–559 (1993). doi: 10.1086/173334
- Y.W. Lee, On the Sandage period shift effect among field RR Lyrae stars. *Astrophys. J.* **363**, 159–167 (1990). doi: 10.1086/169326
- B. Letarte, S.C. Chapman, M. Collins, R.A. Ibata, M.J. Irwin, A.M.N. Ferguson, G.F. Lewis, N. Martin, A. McConnachie, N. Tanvir, A Keck/DEIMOS spectroscopic survey of the faint M31 satellites And XV and And XVI. *Mon. Not. R. Astron. Soc.* **400**, 1472–1478 (2009). doi: 10.1111/j.1365-2966.2009.15546.x
- K. Liao, T. Treu, P. Marshall, C.D. Fassnacht, N. Rumbaugh, G. Dobler, A. Aghamousa, V. Bonvin, F. Courbin, A. Hojjati, N. Jackson, V. Kashyap, S. Rathna Kumar, E. Linder, K. Mandel, X.L. Meng, G. Meylan, L.A. Moustakas, T.P. Prabhu, A. Romero-Wolf, A. Shafieloo, A. Siemiginowska, C.S. Stalin, H. Tak, M. Tewes, D. van Dyk, Strong Lens Time Delay Challenge. II. Results of TDC1. *Astrophys. J.* **800**, 11 (2015). doi: 10.1088/0004-

- 637X/800/1/11
- B.F. Madore, W.L. Freedman, The tip of the red giant branch as a distance indicator for resolved galaxies. II: Computer simulations. *Astron. J.* **109**, 1645–1652 (1995). doi: 10.1086/117391
- Z. Malkin, Statistical analysis of the determinations of the Sun’s Galactocentric distance. In: *Advancing the Physics of Cosmic Distances*, ed. R. de Grijs, *Int’l Astron. Union Symp.* **289**, 406–409 (2013a). doi: 10.1017/S1743921312021825
- Z.M. Malkin, Analysis of determinations of the distance between the sun and the galactic center. *Astron. Rep.* **47**, 128–133 (2013b). doi: 10.1134/S1063772913020078
- M. Marconi, G. Coppola, G. Bono, V. Braga, A. Pietrinferni, R. Buonanno, M. Castellani, I. Musella, V. Ripepi, R.F. Stellingwerf, On a New Theoretical Framework for RR Lyrae Stars. I. The Metallicity Dependence. *Astrophys. J.* **808**, 50 (2015). doi: 10.1088/0004-637X/808/1/50
- P.J. Marshall, D.W. Hogg, L.A. Moustakas, C.D. Fassnacht, M. Bradač, T. Schrabback, R.D. Blandford, Automated Detection of Galaxy-Scale Gravitational Lenses in High-Resolution Imaging Data. *Astrophys. J.* **694**, 924–942 (2009). doi: 10.1088/0004-637X/694/2/924
- P.J. Marshall, A. Verma, A. More, C.P. Davis, S. More, A. Kapadia, M. Parrish, C. Snyder, J. Wilcox, E. Baeten, C. Macmillan, C. Cornen, M. Baumer, E. Simpson, C.J. Lintott, D. Miller, E. Paget, R. Simpson, A.M. Smith, R. Küng, P. Saha, T.E. Collett, SPACE WARPS – I. Crowdsourcing the discovery of gravitational lenses. *Mon. Not. R. Astron. Soc.* **455**, 1171–1190 (2016). doi: 10.1093/mnras/stv2009
- N.F. Martin, D.L. Nidever, G. Besla, K. Olsen, A.R. Walker, A.K. Vivas, R.A. Gruendl, C.C. Kaleida, R.R. Muñoz, R.D. Blum, A. Saha, B.C. Conn, E.F. Bell, Y.H. Chu, M.-R.L. Cioni, T.J.L. de Boer, C. Gallart, S. Jin, A. Kunder, S.R. Majewski, D. Martínez-Delgado, A. Monachesi, M. Monelli, L. Montegudo, N.E.D. Noël, E.W. Olszewski, G.S. Stringfellow, R.P. van der Marel, D. Zaritsky, Hydra II: a faint and compact Milky Way dwarf galaxy found in the Survey of the Magellanic Stellar History. *Astrophys. J.* **804**, L5 (2015). doi: 10.1088/2041-8205/804/1/L5
- C.E. Martínez-Vázquez, M. Monelli, G. Bono, P.B. Stetson, I. Ferraro, E.J. Bernard, C. Gallart, G. Fiorentino, G. Iannicola, A. Udalski, Variable stars in Local Group Galaxies – I. Tracing the early chemical enrichment and radial gradients in the Sculptor dSph with RR Lyrae stars. *Mon. Not. R. Astron. Soc.* **454**, 1509–1516 (2015). doi: 10.1093/mnras/stv2014
- C.E. Martínez-Vázquez, P.B. Stetson, M. Monelli, E.J. Bernard, G. Fiorentino, C. Gallart, G. Bono, S. Cassisi, M. Dall’Ora, I. Ferraro, G. Iannicola, A.R. Walker, Variable stars in Local Group Galaxies – II. Sculptor dSph. *Mon. Not. R. Astron. Soc.* **462**, 4349–4370 (2016). doi: 10.1093/mnras/stw1895
- M.L. Mateo, Dwarf Galaxies of the Local Group. *Annu. Rev. Astron. Astrophys.* **36**, 435–506 (1998). doi: 10.1146/annurev.astro.36.1.435
- A.W. McConnachie, The Observed Properties of Dwarf Galaxies in and around the Local Group. *Astron. J.* **144**, 4 (2012). doi: 10.1088/0004-6256/144/1/4

- A.W. McConnachie, M.J. Irwin, A.M.N. Ferguson, R.A. Ibata, G.F. Lewis, N. Tanvir, Determining the location of the tip of the red giant branch in old stellar populations: M33, Andromeda I and II. *Mon. Not. R. Astron. Soc.* **350**, 243–252 (2004). doi: 10.1111/j.1365-2966.2004.07637.x
- A.W. McConnachie, M.J. Irwin, A.M.N. Ferguson, R.A. Ibata, G.F. Lewis, N. Tanvir, Distances and metallicities for 17 Local Group galaxies. *Mon. Not. R. Astron. Soc.* **356**, 979–997 (2005). doi: 10.1111/j.1365-2966.2004.08514.x
- A.W. McConnachie, M.J. Irwin, R.A. Ibata, J. Dubinski, L.M. Widrow, N.F. Martin, P. Côté, A.L. Dotter, J.F. Navarro, A.M.N. Ferguson, T.H. Puzia, G.F. Lewis, A. Babul, P. Barmby, O. Bienaymé, S.C. Chapman, R. Cockcroft, M.L.M. Collins, M.A. Fardal, W.E. Harris, A. Huxor, A.D. Mackey, J. Peñarrubia, R.M. Rich, H.B. Richer, A. Siebert, N. Tanvir, D. Valls-Gabaud, K.A. Venn, The remnants of galaxy formation from a panoramic survey of the region around M31. *Nature* **461**, 66–69 (2009). doi: 10.1038/nature08327
- A.W. McConnachie, The Observed Properties of Dwarf Galaxies in and around the Local Group. *Astron. J.* **144**, 4 (2012). doi: 10.1088/0004-6256/144/1/4
- C. McCully, C.R. Keeton, K.C. Wong, A.I. Zabludoff, A new hybrid framework to efficiently model lines of sight to gravitational lenses. *Mon. Not. R. Astron. Soc.* **443**, 3631–3642 (2014). doi: 10.1093/mnras/stu1316
- C. McCully, C.R. Keeton, K.C. Wong, A.I. Zabludoff, Quantifying Environmental and Line-of-Sight Effects in Models of Strong Gravitational Lens Systems. *Astrophys. J.* **836**, 141 (2017). doi: 10.3847/1538-4357/836/1/141
- K.B.W. McQuinn, E.D. Skillman, A. Dolphin, J.M. Cannon, J.J. Salzer, K.L. Rhode, E.A.K. Adams, D. Berg, R. Giovanelli, L. Girardi, M.P. Haynes, Leo P: An Unquenched Very Low-mass Galaxy. *Astrophys. J.* **812**, 158 (2015). doi: 10.1088/0004-637X/812/2/158
- X.L. Meng, T. Treu, A. Agnello, M.W. Auger, K. Liao, P.J. Marshall, Precision cosmology with time delay lenses: high resolution imaging requirements. *J. Cosmol. Astropart. Phys.* **2015**(09), 059, doi: 10.1088/1475-7516/2015/09/059
- S. Miyazaki, Y. Komiyama, H. Nakaya, Y. Kamata, Y. Doi, T. Hamana, H. Karoji, H. Furusawa, S. Kawanomoto, T. Morokuma, Y. Ishizuka, K. Nariai, Y. Tanaka, F. Uraguchi, Y. Utsumi, Y. Obuchi, Y. Okura, M. Oguri, T. Takata, D. Tomono, T. Kurakami, K. Namikawa, T. Usuda, H. Yamanoi, T. Terai, H. Uekiyo, Y. Yamada, M. Koike, H. Aihara, Y. Fujimori, S. Mineo, H. Miyatake, N. Yasuda, J. Nishizawa, T. Saito, M. Tanaka, T. Uchida, N. Katayama, S.Y. Wang, H.Y. Chen, R. Lupton, C. Loomis, S. Bickerton, P. Price, J. Gunn, H. Suzuki, Y. Miyazaki, M. Muramatsu, K. Yamamoto, M. Endo, Y. Ezaki, N. Itoh, Y. Miwa, H. Yokota, T. Matsuda, R. Ebinuma, K. Takeshi, Hyper Suprime-Cam. In: *SPIE Conf. Ser.*, **8446**, 84460Z, doi: 10.1117/12.926844
- M. Monelli, C. Gallart, S.L. Hidalgo, A. Aparicio, E.D. Skillman, A.A. Cole, D.R. Weisz, L. Mayer, E.J. Bernard, S. Cassisi, A.E. Dolphin, I. Drozdovsky, P.B. Stetson, The ACS LCID Project. VI. The Star Formation History of The Tucana dSph and The Relative Ages of the Isolated dSph Galaxies. *Astrophys. J.* **722**, 1864–1878 (2010a). doi: 10.1088/0004-637X/722/2/1864

- M. Monelli, S.L. Hidalgo, P.B. Stetson, A. Aparicio, C. Gallart, A.E. Dolphin, A.A. Cole, D.R. Weisz, E.D. Skillman, E.J. Bernard, L. Mayer, J.F. Navarro, S. Cassisi, I. Drozdovsky, E. Tolstoy, The ACS LCID Project. III. The Star Formation History of the Cetus dSph Galaxy: A Post-reionization Fossil. *Astrophys. J.* **720**, 1225–1245 (2010b). doi: 10.1088/0004-637X/720/2/1225
- M. Monelli, E.J. Bernard, C. Gallart, G. Fiorentino, I. Drozdovsky, A. Aparicio, G. Bono, S. Cassisi, E.D. Skillman, P.B. Stetson, Variable stars in the Cetus dwarf spheroidal galaxy: population gradients and connections with the star formation history. *Mon. Not. R. Astron. Soc.* **422**, 89–105 (2012). doi: 10.1111/j.1365-2966.2012.20539.x
- M. Monelli, C.E. Martínez-Vázquez, E.J. Bernard, C. Gallart, E.D. Skillman, D.R. Weisz, A.E. Dolphin, S.L. Hidalgo, A.A. Cole, N.F. Martin, A. Aparicio, S. Cassisi, M. Boylan-Kolchin, L. Mayer, A. McConnachie, K.B.W. McQuinn, J.F. Navarro, The ISLANDS Project. I. Andromeda XVI, An Extremely Low Mass Galaxy Not Quenched by Reionization. *Astrophys. J.* **819**, 147 (2016). doi: 10.3847/0004-637X/819/2/147
- A. More, M. Oguri, I. Kayo, J. Zinn, M.A. Strauss, B.X. Santiago, A.M. Mosquera, N. Inada, C.S. Kochanek, C.E. Rusu, J.R. Brownstein, L.N. da Costa, J.P. Kneib, M.A.G. Maia, R.M. Quimby, D.P. Schneider, A. Streblyanska, D.G. York, The SDSS-III BOSS quasar lens survey: discovery of 13 gravitationally lensed quasars. *Mon. Not. R. Astron. Soc.* **456**, 1595–1606 (2016a). doi: 10.1093/mnras/stv2813
- A. More, A. Verma, P.J. Marshall, S. More, E. Baeten, J. Wilcox, C. Macmillan, C. Cornen, A. Kapadia, M. Parrish, C. Snyder, C.P. Davis, R. Gavazzi, C.J. Lintott, R. Simpson, D. Miller, A.M. Smith, E. Paget, P. Saha, R. Küng, T.E. Collett, SPACE WARPS – II. New gravitational lens candidates from the CFHTLS discovered through citizen science. *Mon. Not. R. Astron. Soc.* **455**, 1191–1210 (2016b). doi: 10.1093/mnras/stv1965
- J. Mould, J. Kristian, The dwarf spheroidal galaxy Andromeda I. *Astrophys. J.* **354**, 438–445 (1990). doi: 10.1086/168706
- R.F. Mushotzky, R. Edelson, W. Baumgartner, P. Gandhi, Kepler Observations of Rapid Optical Variability in Active Galactic Nuclei. *Astrophys. J. Lett.* **743**, L12 (2011) doi: 10.1088/2041-8205/743/1/L12
- S.T. Myers, N.J. Jackson, I.W.A. Browne, A.G. de Bruyn, T.J. Pearson, A.C.S. Readhead, P.N. Wilkinson, A.D. Biggs, R.D. Blandford, C.D. Fassnacht, L.V.E. Koopmans, D.R. Marlow, J.P. McKean, M.A. Norbury, P.M. Phillips, D. Rusin, M.C. Shepherd, C.M. Sykes, The Cosmic Lens All-Sky Survey – I. Source selection and observations. *Mon. Not. R. Astron. Soc.* **341**, 1–12 (2003). doi: 10.1046/j.1365-8711.2003.06256.x
- N.R. Napolitano, G. Covone, N. Roy, C. Tortora, F. La Barbera, M. Radovich, F. Getman, M. Capaccioli, A. Colonna, M. Paolillo, G.A. Verdoes Kleijn, L.V.E. Koopmans, KiDS collaboration, Strong lens search in the ESO public Survey KiDS. *Astrophys. Space Sci. Proc.* **42**, 129–134 (2016). doi: 10.1007/978-3-319-19330-4_20
- D.L. Nidever, A. Monachesi, E.F. Bell, S.R. Majewski, R.R. Muñoz, R.L. Beaton, A Tidally Stripped Stellar Component of the Magellanic Bridge.

- Astrophys. J. **779**, 145 (2013). doi: 10.1088/0004-637X/779/2/145
- J.W. Nightingale, S. Dye, Adaptive semi-linear inversion of strong gravitational lens imaging. *Mon. Not. R. Astron. Soc.* **452**, 2940–2959 (2015). doi: 10.1093/mnras/stv1455
- I. Nikiforov, The Distance to the Center of the Galaxy: the Current State-of-the-Art in Measuring R_0 . In: *Order and Chaos in Stellar and Planetary Systems*, G.G. Byrd, K.V. Kholshevnikov, A.A. Myllri, I.I. Nikiforov, V.V. Orlov (eds), *Astron. Soc. Pac. Conf. Proc.* **316**, 199–208 (2004).
- M. Oguri, The Mass Distribution of SDSS J1004+4112 Revisited. *Publ. Astron. Soc. Jpn* **62**, 1017–1024 (2010). doi: 10.1093/pasj/62.4.1017
- M. Oguri, Measuring the distance-redshift relation with the cross-correlation of gravitational wave standard sirens and galaxies. *Phys. Rev. D* **93**, 083511 (2016). doi: 10.1103/PhysRevD.93.083511
- M. Oguri, P.J. Marshall, Gravitationally lensed quasars and supernovae in future wide-field optical imaging surveys. *Mon. Not. R. Astron. Soc.* **405**, 2579–2593 (2010). doi: 10.1111/j.1365-2966.2010.16639.x
- M. Oguri, N. Inada, B. Pindor, M.A. Strauss, G.T. Richards, J.F. Hennawi, E.L. Turner, R.H. Lupton, D.P. Schneider, M. Fukugita, J. Brinkmann, The Sloan Digital Sky Survey Quasar Lens Search. I. Candidate Selection Algorithm. *Astron. J.* **132**, 999–1013 (2006). doi: 10.1086/506019
- M. Oguri, N. Inada, M.A. Strauss, C.S. Kochanek, I. Kayo, M.S. Shin, T. Morokuma, G.T. Richards, C.E. Rusu, J.A. Frieman, M. Fukugita, D.P. Schneider, D.G. York, N.A. Bahcall, R.L. White, The Sloan Digital Sky Survey Quasar Lens Search. VI. Constraints on Dark Energy and the Evolution of Massive Galaxies. *Astron. J.* **143**, 120 (2012). doi: 10.1088/0004-6256/143/5/120
- A.J. Ordoñez, A. Sarajedini, Population Effects on the Metallicity Distribution Function Derived from the Red Giant Branch. *Astron. J.* **149**, 201 (2015). doi: 10.1088/0004-6256/149/6/201
- A.J. Ordoñez, A. Sarajedini, The pulsating variable star population in DDO210. *Mon. Not. R. Astron. Soc.* **455**, 2163–2177 (2016). doi: 10.1093/mnras/stv2494
- A.J. Ordoñez, S.C. Yang, A. Sarajedini, The RR Lyrae Variable Population in the Phoenix Dwarf Galaxy. *Astrophys. J.* **786**, 147 (2014). doi: 10.1088/0004-637X/786/2/147
- F. Ostrovski, R.G. McMahon, A.J. Connolly, C.A. Lemon, M.W. Auger, M. Banerji, J.M. Hung, S.E. Koposov, C.E. Lidman, S.L. Reed, S. Allam, A. Benoit-Lévy, E. Bertin, D. Brooks, E. Buckley-Geer, A. Carnero Rosell, M. Carrasco Kind, J. Carretero, C.E. Cunha, L.N. da Costa, S. Desai, H.T. Diehl, J.P. Dietrich, A.E. Evrard, D.A. Finley, B. Flaugher, P. Fosalba, J. Frieman, D.W. Gerdes, D.A. Goldstein, D. Gruen, R.A. Gruendl, G. Gutierrez, K. Honscheid, D.J. James, K. Kuehn, N. Kuropatkin, M. Lima, H. Lin, M.A.G. Maia, J.L. Marshall, P. Martini, P. Melchior, R. Miquel, R. Ogando, A. Plazas Malagón, K. Reil, K. Romer, E. Sanchez, B. Santiago, V. Scarpine, I. Sevilla-Noarbe, M. Soares-Santos, F. Sobreira, E. Suchyta, G. Tarle, D. Thomas, D.L. Tucker, A.R. Walker, VDES J2325-5229 a $z =$

- 2.7 gravitationally lensed quasar discovered using morphology independent supervised machine learning. *Mon. Not. R. Astron. Soc.* **465**, 4325–4334 (2017). doi: 10.1093/mnras/stw2958
- D. Paraficz, J. Hjorth, Gravitational lenses as cosmic rulers: Ω_m , Ω_Λ from time delays and velocity dispersions. *Astron. Astrophys.* **507**, L49–L52 (2009). doi: 10.1051/0004-6361/200913307
- D. Paraficz, F. Courbin, A. Tramacere, R. Joseph, R.B. Metcalf, J.P. Kneib, P. Dubath, D. Droz, F. Filleul, D. Ringeisen, C. Schäfer, The PCA Lens-Finder: application to CFHTLS. *Astron. Astrophys.* **592**, A75 (2016). doi: 10.1051/0004-6361/201527971
- A. Pietrinferni, S. Cassisi, M. Salaris, F. Castelli, A Large Stellar Evolution Database for Population Synthesis Studies. I. Scaled Solar Models and Isochrones. *Astrophys. J.* **612**, 168–190 (2004). doi: 10.1086/422498
- G. Pietrzyński, D. Graczyk, W. Gieren, I.B. Thompson, B. Pilecki, A. Udalski, I. Soszyński, S. Kozłowski, P. Konorski, K. Suchomska, G. Bono, P.G.P. Moroni, S. Villanova, N. Nardetto, F. Bresolin, R.P. Kudritzki, J. Storm, A. Gellenne, R. Smolec, D. Minniti, M. Kubiak, M.K. Szymański, R. Poleski, L. Wyrzykowski, K. Ulaczyk, P. Pietrukowicz, M. Górski, P. Karczmarek, An eclipsing-binary distance to the Large Magellanic Cloud accurate to two per cent. *Nature* **495**, 76–79 (2013). doi: 10.1038/nature11878
- C.J. Pritchett, S. van den Bergh, Observations of RR Lyrae stars in the halo of M31. *Astrophys. J.* **316**, 517–529 (1987). doi: 10.1086/165223
- B.J. Pritzl, T.E. Armandroff, G.H. Jacoby, G.S. Da Costa, The Dwarf Spheroidal Companions to M31: Variable Stars in Andromeda VI. *Astron. J.* **124**, 1464–1485 (2002a). doi: 10.1086/341823
- B.J. Pritzl, H.A. Smith, M. Catelan, A.V. Sweigart, Variable Stars in the Unusual, Metal-rich Globular Cluster NGC 6388. *Astron. J.* **124**, 949–976 (2002b). doi: 10.1086/341381
- B.J. Pritzl, T.E. Armandroff, G.H. Jacoby, G.S. Da Costa, The Dwarf Spheroidal Companions to M31: Variable Stars in Andromeda II. *Astron. J.* **127**, 318–333 (2004). doi: 10.1086/380613
- B.J. Pritzl, T.E. Armandroff, G.H. Jacoby, G.S. Da Costa, The Dwarf Spheroidal Companions to M31: Variable Stars in Andromeda I and Andromeda III. *Astron. J.* **129**, 2232–2256 (2005a). doi: 10.1086/428372
- B.J. Pritzl, K.A. Venn, M. Irwin, A Comparison of Elemental Abundance Ratios in Globular Clusters, Field Stars, and Dwarf Spheroidal Galaxies. *Astron. J.* **130**, 2140–2165 (2005b) doi: 10.1086/432911
- E.D. Reese, J.E. Carlstrom, M. Joy, J.J. Mohr, L. Grego, W.L. Holzapfel, Determining the Cosmic Distance Scale from Interferometric Measurements of the Sunyaev–Zel’dovich Effect. *Astrophys. J.* **581**, 53–85 (2002). doi: 10.1086/344137
- S. Refsdal, On the possibility of determining Hubble’s parameter and the masses of galaxies from the gravitational lens effect. *Mon. Not. R. Astron. Soc.* **128**, 307–310 (1964). doi: 10.1093/mnras/128.4.307
- M.J. Reid, The Distance to the Galactic Center: R_0 . In: The Center of the Galaxy, ed. M. Morris, Int’l Astron. Union Symp. **136**, 37–46 (1989).

- M.J. Reid, The distance to the center of the Galaxy. *Annu. Rev. Astron. Astrophys.* **31**, 345–372 (1993). doi: 10.1146/annurev.aa.31.090193.002021
- M.J. Reid, J.A. Braatz, J.J. Condon, L.J. Greenhill, C. Henkel, K.Y. Lo, The Megamaser Cosmology Project. I. Very Long Baseline Interferometric Observations of UGC 3789. *Astrophys. J.* **695**, 287–291 (2009). doi: 10.1088/0004-637X/695/1/287
- M.J. Reid, J.A. Braatz, J.J. Condon, K.Y. Lo, C.Y. Kuo, C.M.V. Impellizzeri, C. Henkel, The Megamaser Cosmology Project. IV. A Direct Measurement of the Hubble Constant from UGC 3789. *Astrophys. J.* **767**, 154 (2013). doi: 10.1088/0004-637X/767/2/154
- J.A. Rich, S.E. Persson, W.L. Freedman, B.F. Madore, A.J. Monson, V. Scowcroft, M. Seibert, A New Cepheid Distance Measurement and Method for NGC 6822. *Astrophys. J.* **794**, 107 (2014). doi: 10.1088/0004-637X/794/2/107
- A.G. Riess, L.M. Macri, S.L. Hoffmann, D. Scolnic, S. Casertano, A.V. Filippenko, B.E. Tucker, M.J. Reid, D.O. Jones, J.M. Silverman, R. Chornock, P. Challis, W. Yuan, P.J. Brown, R.J. Foley, A 2.4% Determination of the Local Value of the Hubble Constant. *Astrophys. J.* **826**, 56 (2016). doi: 10.3847/0004-637X/826/1/56
- V. Ripepi, M.I. Moretti, M. Marconi, G. Clementini, M.-R.L. Cioni, J.B. Marquette, L. Girardi, S. Rubele, M.A.T. Groenewegen, R. de Grijs, B.K. Gibson, J.M. Oliveira, J.T. van Loon, J.P. Emerson, The VMC survey – V. First results for classical Cepheids. *Mon. Not. R. Astron. Soc.* **424**, 1807–1816 (2012). doi:10.1111/j.1365-2966.2012.21274.x
- L. Rizzi, E.V. Held, I. Saviane, R.B. Tully, M. Gullieuszik, The distance to the Fornax dwarf spheroidal galaxy. *Mon. Not. R. Astron. Soc.* **380**, 1255–1260 (2007). doi: 10.1111/j.1365-2966.2007.12196.x
- S. Rubele, L. Kerber, L. Girardi, M.-R. Cioni, P. Marigo, S. Zaggia, K. Bekki, R. de Grijs, J. Emerson, M.A.T. Groenewegen, M. Gullieuszik, V. Ivanov, B. Miszalski, J.M. Oliveira, B. Tatton, J.T. van Loon, The VMC survey. IV. The LMC star formation history and disk geometry from four VMC tiles. *Astron. Astrophys.* **537**, A106 (2012). doi: 10.1051/0004-6361/201117863
- S. Rubele, L. Girardi, L. Kerber, M.-R.L. Cioni, A.E. Piatti, S. Zaggia, K. Bekki, A. Bressan, G. Clementini, R. de Grijs, J.P. Emerson, M.A.T. Groenewegen, V.D. Ivanov, M. Marconi, P. Marigo, M.-I. Moretti, V. Ripepi, S. Subramanian, B.L. Tatton, J.T. van Loon, The VMC survey - XIV. First results on the look-back time star formation rate tomography of the Small Magellanic Cloud. *Mon. Not. R. Astron. Soc.* **449**, 639–661 (2015). doi: 10.1093/mnras/stv141
- C.E. Rusu, C.D. Fassnacht, D. Sluse, S. Hilbert, K.C. Wong, K.H. Huang, S.H. Suyu, T.E. Collett, P.J. Marshall, T. Treu, L.V.E. Koopmans, H0LiCOW III. Quantifying the effect of mass along the line of sight to the gravitational lens HE 0435-1223 through weighted galaxy counts. *Mon. Not. R. Astron. Soc.* **467**, 4220–4242 (2017). doi: 10.1093/mnras/stx285
- C.E. Rusu, M. Oguri, Y. Minowa, M. Iye, N. Inada, S. Oya, I. Kayo, Y. Hayano, M. Hattori, Y. Saito, M. Ito, T.S. Pyo, H. Terada, H. Takami, M.

- Watanabe, Subaru Telescope adaptive optics observations of gravitationally lensed quasars in the Sloan Digital Sky Survey. *Mon. Not. R. Astron. Soc.* **458**, 2–55 (2016). doi: 10.1093/mnras/stw092
- M. Rybak, J.P. McKean, S. Vegetti, P. Andreani, S.D.M. White, ALMA imaging of SDP.81 – I. A pixelated reconstruction of the far-infrared continuum emission. *Mon. Not. R. Astron. Soc.* **451**, L40–L44 (2015). doi: 10.1093/mnrasl/slv058
- A. Saha, J.G. Hoessel, RR Lyrae stars in local group galaxies. I – NGC 185. *Astron. J.* **99**, 97–148 (1990). doi: 10.1086/115316
- A. Saha, J.G. Hoessel, A.E. Mossman, RR Lyrae stars in local group galaxies. II – NGC 147. *Astron. J.* **100**, 108–126 (1990). doi: 10.1086/115495
- M. Salaris, A. Weiss, Homogeneous age dating of 55 Galactic globular clusters. Clues to the Galaxy formation mechanisms. *Astron. Astrophys.* **388**, 492–503 (2002). doi: 10.1051/0004-6361:20020554
- L.V. Sales, J.F. Navarro, M.G. Abadi, M. Steinmetz, Cosmic ménage à trois: the origin of satellite galaxies on extreme orbits. *Mon. Not. R. Astron. Soc.* **379**, 1475–1483 (2007). doi: 10.1111/j.1365-2966.2007.12026.x
- A. Sandage, The Oosterhoff period–metallicity relation for RR Lyrae stars at the blue fundamental edge of the instability strip. *Astron. J.* **106**, 687–702 (1993). doi: 10.1086/116675
- A. Sarajedini, M.K. Barker, D. Geisler, P. Harding, R. Schommer, RR Lyrae Variables in M33. I. Evidence for a Field Halo Population. *Astron. J.* **132**, 1361–1371 (2006). doi: 10.1086/506152
- A. Sarajedini, S.C. Yang, A. Monachesi, T.R. Lauer, S.C. Trager, An ancient metal-poor population in M32, and halo satellite accretion in M31, identified by RR Lyrae stars. *Mon. Not. R. Astron. Soc.* **425**, 1459–1472 (2012). doi: 10.1111/j.1365-2966.2012.21609.x
- B.E. Schaefer, A Problem with the Clustering of Recent Measures of the Distance to the Large Magellanic Cloud. *Astron. J.* **135**, 112–119 (2008). doi: 10.1088/0004-6256/135/1/112
- B.E. Schaefer, An accurate distance to the nearest galaxy. *Nature*, **495**, 51–52 (2013). doi: 10.1038/495051a
- P.L. Schechter, N.D. Morgan, B. Chehade, N. Metcalfe, T. Shanks, M. McDonald, First lensed quasar system(s) from the VST-ATLAS survey: one quad and three nearly identical pairs. *Astron. J.*, in press (arXiv:1607.07476) (2017).
- E.F. Schlafly, D.P. Finkbeiner, Measuring Reddening with Sloan Digital Sky Survey Stellar Spectra and Recalibrating SFD. *Astrophys. J.* **737**, 103 (2011). doi: 10.1088/0004-637X/737/2/103
- D.J. Schlegel, D.P. Finkbeiner, M. Davis, Maps of Dust Infrared Emission for Use in Estimation of Reddening and Cosmic Microwave Background Radiation Foregrounds. *Astrophys. J.* **500**, 525–553 (1998). doi: 10.1086/305772
- P. Schneider, D. Sluse, Mass-sheet degeneracy, power-law models and external convergence: Impact on the determination of the Hubble constant from gravitational lensing. *Astron. Astrophys.* **559**, A37 (2013). doi: 10.1051/0004-6361/201321882

- P. Schneider, D. Sluse, Source-position transformation: an approximate invariance in strong gravitational lensing. *Astron. Astrophys.* **564**, A103 (2014). doi: 10.1051/0004-6361/201322106
- B.F. Schutz, Determining the Hubble constant from gravitational wave observations. *Nature* **323**, 310–311 (1986). doi: 10.1038/323310a0
- V. Scowcroft, W.L. Freedman, B.F. Madore, A.J. Monson, S.E. Persson, M. Seibert, J.R. Rigby, J. Melbourne, The Carnegie Hubble Program: The Infrared Leavitt Law in IC 1613. *Astrophys. J.* **773**, 106 (2013). doi: 10.1088/0004-637X/773/2/106
- V. Scowcroft, W.L. Freedman, B.F. Madore, A. Monson, S.E. Persson, J. Rich, M. Seibert, J.R. Rigby, The Carnegie Hubble Program: The Distance and Structure of the SMC as Revealed by Mid-infrared Observations of Cepheids. *Astrophys. J.* **816**, 49 (2016). doi: 10.3847/0004-637X/816/2/49
- Y. Shu, A.S. Bolton, C.S. Kochanek, M. Oguri, I. Pérez-Fournon, Z. Zheng, S. Mao, A.D. Montero-Dorta, J.R. Brownstein, R. Marques-Chaves, B. Ménard, The BOSS Emission-line Lens Survey. III. Strong Lensing of Ly α Emitters by Individual Galaxies. *Astrophys. J.* **824**, 86 (2016). doi: 10.3847/0004-637X/824/2/86
- J. Silk, S.D.M. White, The determination of Q_0 using X-ray and microwave observations of galaxy clusters. *Astrophys. J. Lett.* **226**, L103–L106 (1978). doi: 10.1086/182841
- M. Sirianni, M.J. Jee, N. Benítez, J.P. Blakeslee, A.R. Martel, G. Meurer, M. Clampin, G. De Marchi, H.C. Ford, R. Gilliland, G.F. Hartig, G.D. Illingworth, J. Mack, W.J. McCann, The Photometric Performance and Calibration of the Hubble Space Telescope Advanced Camera for Surveys. *Publ. Astron. Soc. Pac.* **117**, 1049–1112 (2005). doi: 10.1086/444553
- E.D. Skillman, M. Monelli, D.R. Weisz, S.L. Hidalgo, A. Aparicio, E.J. Bernard, M. Boylan-Kolchin, S. Cassisi, A.A. Cole, A.E. Dolphin, H.C. Ferguson, C. Gallart, M.J. Irwin, N.F. Martin, C.E. Martínez-Vázquez, L. Mayer, A.W. McConnachie, K.B.W. McQuinn, J.F. Navarro, P.B. Stetson, The ISLANDS project II: The Lifetime Star Formation Histories of Six Andromeda dSphs. *Astrophys. J.* **837**, 102 (2017). doi: 10.3847/1538-4357/aa60c5
- C.T. Slater, E.F. Bell, N.F. Martin, E.J. Tollerud, N. Ho, A Deep Study of the Dwarf Satellites Andromeda XXVIII and Andromeda XXIX. *Astrophys. J.* **806**, 230 (2015). doi: 10.1088/0004-637X/806/2/230
- D. Sluse, A. Sonnenfeld, N. Rumbaugh, C.E. Rusu, C.D. Fassnacht, T. Treu, S.H. Suyu, K.C. Wong, M.W. Auger, V. Bonvin, T. Collett, F. Courbin, S. Hilbert, L.V.E. Koopmans, P.J. Marshall, G. Meylan, C. Spiniello, M. Tewes, H0LiCOW II. Spectroscopic survey and galaxy-group identification of the strong gravitational lens system HE0435–1223. *Mon. Not. R. Astron. Soc.*, submitted (arXiv:1607.00382) (2016).
- H.A. Smith, RR Lyrae stars. *Cambridge Astrophys. Ser.*, 27 (Cambridge, UK: Cambridge Univ. Press) (1995).
- A. Sonnenfeld, J.H.H. Chan, Y. Shu, A. More, M. Oguri, S.H. Suyu, K.C. Wong, C.-H. Lee, J. Coupon, A. Yonehara, A.S. Bolton, A.T. Jaelani, M.

- Tanaka, S. Miyazaki, Y. Komiyama, Survey of Gravitationally-lensed Objects in HSC Imaging (SuGOHI). I. Automatic search for galaxy-scale strong lenses. *Publ. Astron. Soc. Jpn*, submitted (arXiv:1704.01585) (2017).
- I. Soszyński, A. Udalski, M.K. Szymański, M. Kubiak, G. Pietrzyński, L. Wyrzykowski, O. Szewczyk, K. Ulaczyk, R. Poleski, The Optical Gravitational Lensing Experiment. The OGLE-III Catalog of Variable Stars. II. Type II Cepheids and Anomalous Cepheids in the Large Magellanic Cloud. *Acta Astron.* **58**, 293–312 (2008).
- I. Soszyński, A. Udalski, M.K. Szymański, L. Wyrzykowski, K. Ulaczyk, R. Poleski, P. Pietrukowicz, S. Kozłowski, D.M. Skowron, J. Skowron, P. Mróz, M. Pawlak, The OGLE Collection of Variable Stars. Over 45 000 RR Lyrae Stars in the Magellanic System. *Acta Astron.* **66**, 131–147 (2016).
- P.B. Stetson, Homogeneous Photometry for Star Clusters and Resolved Galaxies. II. Photometric Standard Stars. *Publ. Astron. Soc. Pac.* **112**, 925–931 (2000). doi: 10.1086/316595
- P.B. Stetson, G. Fiorentino, G. Bono, E.J. Bernard, M. Monelli, G. Iannicola, C. Gallart, I. Ferraro, Homogeneous Photometry. VI: Variable Stars in the Leo I Dwarf Spheroidal Galaxy. *Publ. Astron. Soc. Pac.* **126**, 616–641 (2014). doi: 10.1086/677352
- S. Subramanian, A. Subramaniam, The Three-dimensional Structure of the Small Magellanic Cloud. *Astrophys. J.* **744**, 128 (2012). doi: 10.1088/0004-637X/744/2/128
- S. Subramanian, A. Subramaniam, Disk of the Small Magellanic Cloud as traced by Cepheids. *Astron. Astrophys.* **573**, A135 (2015). doi: 10.1051/0004-6361/201424248
- S.H. Suyu, A. Halkola, The halos of satellite galaxies: the companion of the massive elliptical lens SL2S J08544–0121. *Astron. Astrophys.* **524**, A94 (2010). doi: 10.1051/0004-6361/201015481
- S.H. Suyu, P.J. Marshall, M.P. Hobson, R.D. Blandford, A Bayesian analysis of regularized source inversions in gravitational lensing. *Mon. Not. R. Astron. Soc.* **371**, 983–998 (2006). doi: 10.1111/j.1365-2966.2006.10733.x
- S.H. Suyu, P.J. Marshall, R.D. Blandford, C.D. Fassnacht, L.V.E. Koopmans, J.P. McKean, T. Treu, Dissecting the Gravitational Lens B1608+656. I. Lens Potential Reconstruction. *Astrophys. J.* **691**, 277–298 (2009). doi: 10.1088/0004-637X/691/1/277
- S.H. Suyu, P.J. Marshall, M.W. Auger, S. Hilbert, R.D. Blandford, L.V.E. Koopmans, C.D. Fassnacht, T. Treu, Dissecting the Gravitational lens B1608+656. II. Precision Measurements of the Hubble Constant, Spatial Curvature, and the Dark Energy Equation of State. *Astrophys. J.* **711**, 201–221 (2010). doi: 10.1088/0004-637X/711/1/201
- S.H. Suyu, M.W. Auger, S. Hilbert, P.J. Marshall, M. Tewes, T. Treu, C.D. Fassnacht, L.V.E. Koopmans, D. Sluse, R.D. Blandford, F. Courbin, G. Meylan, Two Accurate Time-delay Distances from Strong Lensing: Implications for Cosmology. *Astrophys. J.* **766**, 70 (2013). doi: 10.1088/0004-637X/766/2/70

- S.H. Suyu, T. Treu, S. Hilbert, A. Sonnenfeld, M.W. Auger, R.D. Blandford, T. Collett, F. Courbin, C.D. Fassnacht, L.V.E. Koopmans, P.J. Marshall, G. Meylan, C. Spiniello, M. Tewes, Cosmology from Gravitational Lens Time Delays and Planck Data. *Astrophys. J. Lett.* **788**, L35 (2014). doi: 10.1088/2041-8205/788/2/L35
- S.H. Suyu, V. Bonvin, F. Courbin, C.D. Fassnacht, C.E. Rusu, D. Sluse, T. Treu, K.C. Wong, M.W. Auger, X. Ding, S. Hilbert, P.J. Marshall, N. Rumbaugh, A. Sonnenfeld, M. Tewes, O. Tihhonova, A. Agnello, R.D. Blandford, G.C.F. Chen, T. Collett, L.V.E. Koopmans, K. Liao, G. Meylan, C. Spiniello, H0LiCOW I. H_0 Lenses in COSMOGRAIL's Wellspring: Program Overview. *Mon. Not. R. Astron. Soc.*, in press (arXiv:1607.00017) (2017).
- A.S. Tagore, N. Jackson, On the use of shapelets in modelling resolved, gravitationally lensed images. *Mon. Not. R. Astron. Soc.* **457**, 3066–3075 (2016). doi: 10.1093/mnras/stw057
- A.S. Tagore, C.R. Keeton, Statistical and systematic uncertainties in pixel-based source reconstruction algorithms for gravitational lensing. *Mon. Not. R. Astron. Soc.* **445**, 694–710 (2014) doi: 10.1093/mnras/stu1671
- G.A. Tammann, A. Sandage, B. Reindl, The expansion field: the value of H_0 . *Astron. Astrophys. Rev.* **15**, 289–331 (2008). doi: 10.1007/s00159-008-0012-y
- M. Tewes, F. Courbin, G. Meylan, C.S. Kochanek, E. Eulaers, N. Cantale, A.M. Mosquera, P. Magain, H. Van Winckel, D. Sluse, G. Cataldi, D. Vörös, S. Dye, COSMOGRAIL: the COSmological MOnitoring of GRAvitational Lenses. XIII. Time delays and 9-yr optical monitoring of the lensed quasar RX J1131–1231. *Astron. Astrophys.* **556**, A22 (2013). doi: 10.1051/0004-6361/201220352
- F. Thévenin, M. Falanga, C.Y. Kuo, G. Pietrzyński, M. Yamaguchi, Modern geometric methods of distance determination. *Space Sci. Rev.*, submitted (2017).
- E.L. Turner, R. Cen, J.P. Ostriker, The relation of local measures of Hubble's constant to its global value. *Astron. J.* **103**, 1427–1437 (1992). doi: 10.1086/116156
- A. Udalski, L. Wyrzykowski, G. Pietrzyński, O. Szweczyk, M. Szymański, M. Kubiak, I. Soszyński, K. Żebruń, The Optical Gravitational Lensing Experiment. Cepheids in the Galaxy IC 1613: No Dependence of the Period–Luminosity Relation on Metallicity. *Acta Astron.* **51**, 221–245 (2001).
- S. van den Bergh, The Galaxies of the Local Group (to be Concluded). *J. R. Astron. Soc. Can.* **62**, 145–180 (1968).
- S. Vegetti, L.V.E. Koopmans, Bayesian strong gravitational-lens modelling on adaptive grids: objective detection of mass substructure in Galaxies. *Mon. Not. R. Astron. Soc.* **392**, 945–963 (2009). doi: 10.1111/j.1365-2966.2008.14005.x
- A.K. Vivas, R. Zinn, J. Farmer, S. Duffau, Y. Ping, Disentangling the Virgo Overdensity with RR Lyrae stars. *Astrophys. J.* **831**, 165 (2016). doi: 10.3847/0004-637X/831/2/165

- A.R. Walker, CCD photometry of the RR Lyrae variables in the LMC cluster NGC 2257 and the adjacent field. *Astron. J.* **98**, 2086–2123 (1989). doi: 10.1086/115282
- A.R. Walker, The Large Magellanic Cloud and the distance scale. *Astrophys. Space Sci.* **341**, 43–49 (2012). doi: 10.1007/s10509-011-0961-x
- S.J. Warren, S. Dye, Semilinear Gravitational Lens Inversion. *Astrophys. J.* **590**, 673–682 (2003). doi: 10.1086/375132
- D.R. Weisz, E.D. Skillman, S.L. Hidalgo, M. Monelli, A.E. Dolphin, A. McConnachie, E.J. Bernard, C. Gallart, A. Aparicio, M. Boylan-Kolchin, S. Cassisi, A.A. Cole, H.C. Ferguson, M. Irwin, N.F. Martin, L. Mayer, K.B.W. McQuinn, J.F. Navarro, P.B. Stetson, Comparing M31 and Milky Way Satellites: The Extended Star Formation Histories of Andromeda II and Andromeda XVI. *Astrophys. J.* **789**, 24 (2014). doi: 10.1088/0004-637X/789/1/24
- B. Willman, M. Masjedi, D.W. Hogg, J.J. Dalcanton, D. Martinez-Delgado, M. Blanton, A.A. West, A. Dotter, B. Chaboyer, Willman 1 – A Galactic Satellite at 40 kpc With Multiple Stellar Tails. arXiv:astro-ph/0603486 (2006).
- K.C. Wong, S.H. Suyu, M.W. Auger, V. Bonvin, F. Courbin, C.D. Fassnacht, A. Halkola, C.E. Rusu, D. Sluse, A. Sonnenfeld, T. Treu, T.E. Collett, S. Hilbert, L.V.E. Koopmans, P.J. Marshall, N. Rumbaugh, H0LiCOW IV. Lens mass model of HE 0435–1223 and blind measurement of its time-delay distance for cosmology. *Mon. Not. R. Astron. Soc.* **465**, 4895–4913 (2017). doi: 10.1093/mnras/stw3077
- P.F. Wu, R.B. Tully, L. Rizzi, A.E. Dolphin, B.A. Jacobs, I.D. Karachentsev, Infrared Tip of the Red Giant Branch and Distances to the Maffei/IC 342 Group. *Astron. J.* **148**, 7 (2014). doi: 10.1088/0004-6256/148/1/7
- O. Wucknitz, A.D. Biggs, I.W.A. Browne, Models for the lens and source of B0218+357: a LENCLEAN approach to determine H_0 . *Mon. Not. R. Astron. Soc.* **349**, 14–30 (2004). doi: 10.1111/j.1365-2966.2004.07514.x
- D. Xu, D. Sluse, P. Schneider, V. Springel, M. Vogelsberger, D. Nelson, L. Hernquist, Lens galaxies in the Illustris simulation: power-law models and the bias of the Hubble constant from time delays. *Mon. Not. R. Astron. Soc.* **456**, 739–755 (2016). doi: 10.1093/mnras/stv2708
- S.C. Yang, A. Sarajedini, HST/WFPC2 imaging of the dwarf satellites And XI and And XIII: horizontal branch morphology and RR Lyraes. *Mon. Not. R. Astron. Soc.* **419**, 1362–1375 (2012). doi: 10.1111/j.1365-2966.2011.19792.x
- S.C. Yang, R. Wagner-Kaiser, A. Sarajedini, S.C. Kim, J. Kyeong, The Early Chemical Enrichment Histories of Two Sculptor Group Dwarf Galaxies as Revealed by RR Lyrae Variables. *Astrophys. J.* **784**, 76 (2014). doi: 10.1088/0004-637X/784/1/76

